AD-A189 627 THERMAL INSTABILITY AND HEAT TRANSFER CHARACTERISTICS IN WATER/ICE SYSTEMS(U) COLD REGIONS RESEARCH AND ENGINEERING LAB HANOVER NH Y YEN NOV 87 CRREL-87-22 1/1

UNCLASSIFIED F/G 8/3 NL

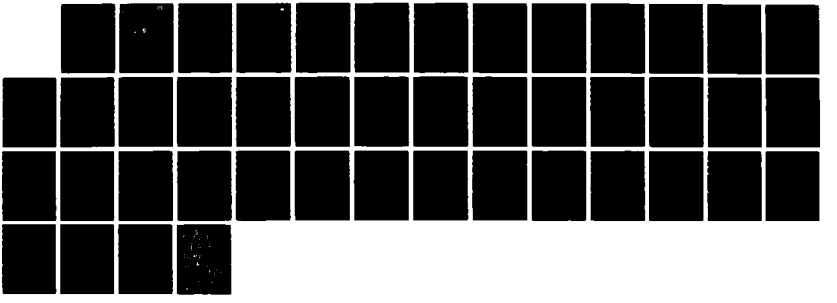

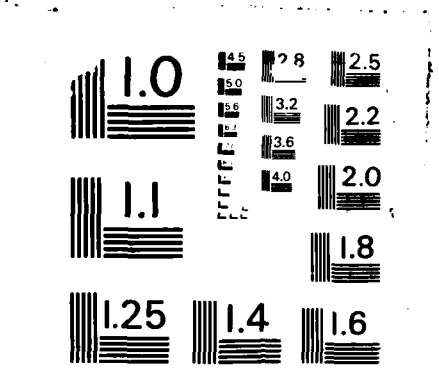

MICROCOPY RESOLUTION TEST CHART

NATIONAL BUREAU OF STANDARDS - 1963 -

CRREL
REPORT 87-22

US Army Corps
of Engineers
Cold Regions Research &
Engineering Laboratory

Thermal instability and heat transfer characteristics in water/ice systems

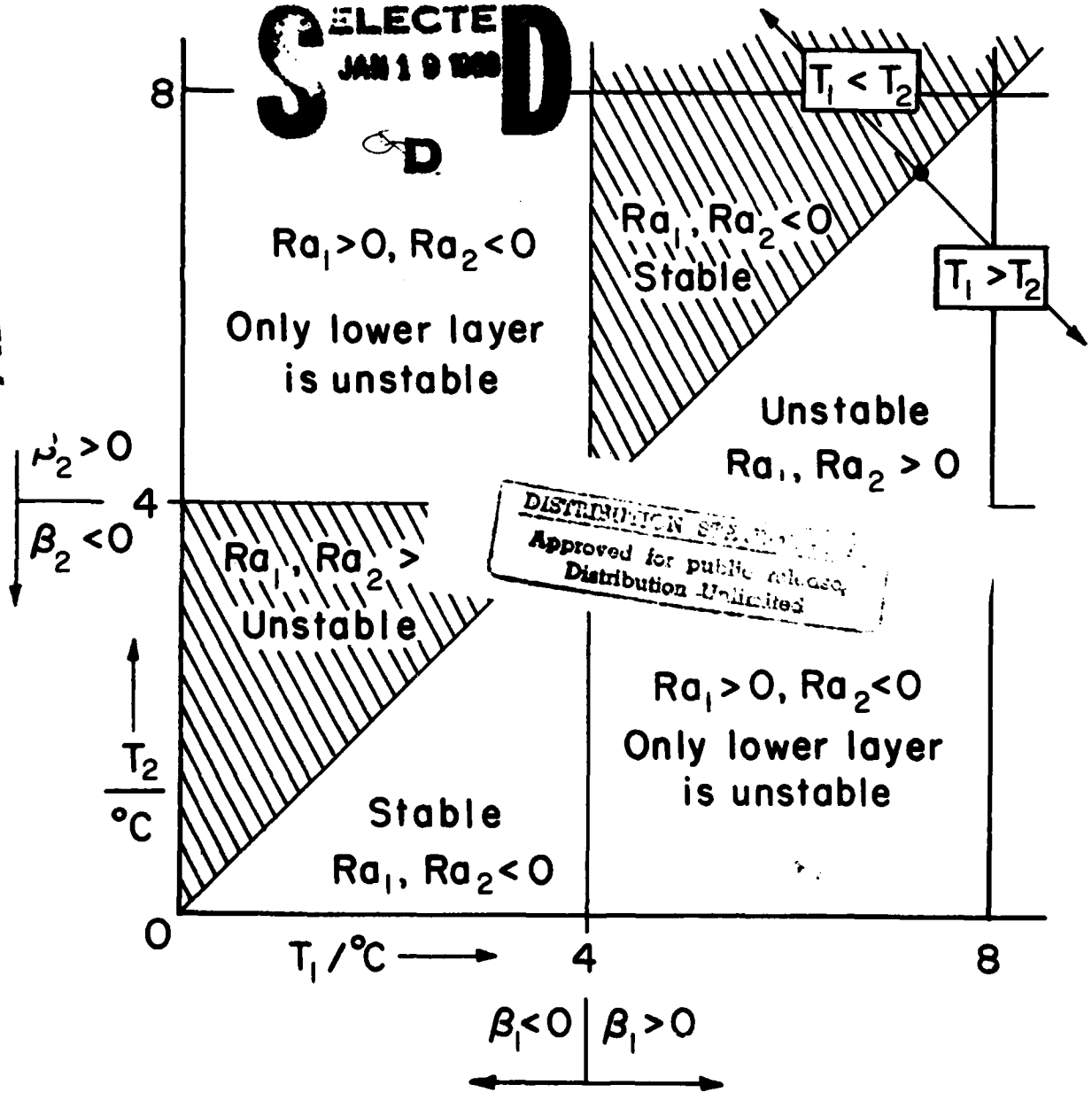

For conversion of SI metric units to U.S./British customary units of measurement consult ASTM Standard E380, Metric Practice Guide, *published by the American Society for Testing and Materials, 1916 Race St., Philadelphia, Pa. 19103.*

Cover: Diagram of fluids stability where β_1 *and* β_2 *are coefficients of thermal expansion evaluated at* T_1 *and* T_2 *respectively and* Ra_1 *and* Ra_2 *are the corresponding Rayleigh numbers.*

CRREL Report 87-22

November 1987

Thermal instability and heat transfer characteristics in water/ice systems

Yin-Chao Yen

Prepared for
OFFICE OF THE CHIEF OF ENGINEERS

Unclassified

SECURITY CLASSIFICATION OF THIS PAGE

REPORT DOCUMENTATION PAGE

Form Approved
OMB No 0704-0188
Exp Date Jun 30, 1986

1a REPORT SECURITY CLASSIFICATION Unclassified	1b RESTRICTIVE MARKINGS
2a SECURITY CLASSIFICATION AUTHORITY	3 DISTRIBUTION / AVAILABILITY OF REPORT Approved for public release; distribution is unlimited.
2b DECLASSIFICATION / DOWNGRADING SCHEDULE	
4 PERFORMING ORGANIZATION REPORT NUMBER(S) CRREL Report 87-22	5 MONITORING ORGANIZATION REPORT NUMBER(S)
6a NAME OF PERFORMING ORGANIZATION U.S. Army Cold Regions Research and Engineering Laboratory 6b OFFICE SYMBOL (*If applicable*) CECRL	7a NAME OF MONITORING ORGANIZATION Office of the CHief of Engineers
6c. ADDRESS (*City, State, and ZIP Code*) Hanover, New Hampshire 03755-1290	7b ADDRESS (*City, State, and ZIP Code*) Washington, D.C. 20314-1000
8a. NAME OF FUNDING / SPONSORING ORGANIZATION 8b OFFICE SYMBOL (*If applicable*)	9. PROCUREMENT INSTRUMENT IDENTIFICATION NUMBER
8c. ADDRESS (*City, State, and ZIP Code*)	10 SOURCE OF FUNDING NUMBERS PROGRAM ELEMENT NO: PROJECT NO 4A1611 02AT24; TASK NO SS; WORK UNIT ACCESSION NO 009

11 TITLE (*Include Security Classification*)
Thermal Instability and Heat Transfer Characteristics in Water/Ice Systems

12 PERSONAL AUTHOR(S)
Yen, Yin-Chao

13a TYPE OF REPORT	13b TIME COVERED FROM ____ TO ____	14 DATE OF REPORT (*Year, Month, Day*)	15 PAGE COUNT
		November 1987	43

16 SUPPLEMENTARY NOTATION

17 COSATI CODES		
FIELD	GROUP	SUB-GROUP

18 SUBJECT TERMS (*Continue on reverse if necessary and identify by block number*)
Density inversion; Natural convection; Heat transfer; Thermal instability; Ice; Water

19 ABSTRACT (*Continue on reverse if necessary and identify by block number*)
This review discusses problems associated with the anomalous temperature-density relations of water. It covers a) onset of convection, b) temperature structure and natural convective heat transfer, and c) laminar forced convective heat transfer in the water/ice system. The onset of convection in a water/ice system was found to be dependent on thermal boundary conditions, not a constant value as in the classical fluids that have a monotonic temperature-density relationship. The water/ice system also exhibits a unique temperature distribution in the melt layer immediately after the critical Rayleigh number is exceeded and soon after it establishes a more or less constant temperature region progressively deepening as the melt layer grows. The constant temperature is approximately 3.2°C for water layers formed from above but varies for melt layers formed from below. The heat flux across the water/ice interface was found to be a weak power function and to increase linearly with temperature for melted layers from above and below, respectively. Both theoretical and experimental melting studies of ice spheres, cylinders, and vertical plates show a minimum heat flux in the water/ice system due to the density extremum of 4°C. The inversion temperature was from 5.1 to 5.6°C. For the case of laminar forced convection melting heat transfer, the presence of an interfacial velocity (due to phase transition) reduces heat transfer in comparison with the case without phase change.

20 DISTRIBUTION / AVAILABILITY OF ABSTRACT	21 ABSTRACT SECURITY CLASSIFICATION	
☒ UNCLASSIFIED/UNLIMITED ☐ SAME AS RPT ☐ DTIC USERS	Unclassified	
22a NAME OF RESPONSIBLE INDIVIDUAL Yin-Chao Yen	22b TELEPHONE (*Include Area Code*) 603-646-4100	22c OFFICE SYMBOL CECRL-EG

DD FORM 1473, 84 MAR

83 APR edition may be used until exhausted
All other editions are obsolete

SECURITY CLASSIFICATION OF THIS PAGE
Unclassified

PREFACE

This report was prepared by Dr. Yin-Chao Yen, Research Physical Scientist, of the Geotechnical Research Branch, Experimental Engineering Division, U.S. Army Cold Regions Research and Engineering Laboratory. The work was performed under DA Project 4A161102 AT24, *Research in Snow, Ice, and Frozen Ground*; Task SS, *Properties of Cold Regions Materials;* Work Unit 009, *Phase Change Thermodynamics in Cold Regions Materials.*

The author thanks Dr. Virgil Lunardini and F. Donald Haynes of CRREL for their constructive review.

CONTENTS

ILLUSTRATIONS

TABLES

NOMENCLATURE

a	wave number, as defined in eq 59
a_N	defined as $\int_0^\infty \exp[-\delta^3 + (\beta\delta/a_N)]d^\delta$
a_o	defined as $\int_0^\infty \exp(-\delta^3)d^\delta$
A	defined as $(T_1 - T_{max})/(T_1 - T_2)$
c_p	specific heat at constant pressure
d	thickness, distance to 4°C front and unstable layer depth
f	factor defined in eq 30
Fo	Fourier number, defined as α_t/ℓ^2
g	gravitational constant
Gr	Grashof number, defined as $(g\beta_\infty\theta_m\ell^3)/\upsilon^2$
h	heat transfer coefficient
H	total layer depth
k	thermal conductivity
k_f	Kutateladze number ($= 1/\beta$)
ℓ	characteristic length
L	latent heat of fusion
m	factor defined in eq 22
n	factor defined in eq 23
N	factor defined in eq 24
Nu	Nusselt number, defined as $h\ell/k$
P_1, P_2, P_3	defined in eq 19, 20, and 21
Pr	Prandtl number, $c_p\mu/k$
q	downward heat flux
Q	defined in eq 8
R	radius
Ra	Rayleigh number, defined in eq 3
S	shape factor, defined in eq 17
St	Stefan number, defined as $[c_p(T_m - T_\infty)]/L$
t	time
T	temperature
ΔT	$T_\infty - T_m$, also $T_1 - T_2$
T^*	defined as $T - T_\infty/T_o - T_\infty$
Ta	Taylor number, defined as $(4\Omega_i^2/\upsilon^2)R_i^4[(1-\mu)(1-\mu/\eta^2)]/(1-\eta^2)^2$
v	fluid velocity
α	thermal diffusivity
β	coefficient of volumetric expansion, also $c_p\Delta T/L$
$\beta_1, \beta_2, \beta_3$	constants in eq 26
β_∞	factor defined in eq 25
γ_1, γ_2	coefficient in eq 2

δ	momentum boundary thickness
δ_t	thermal boundary thickness
δ^{**}	defined in eq 61
δ_t^{**}	defined in eq 60
η	R_1/R_2, y/δ, y/δ_t, or similarity variable defined in eq 55
θ_m	defined as $T_m - T_\infty$
θ_T	defined as h/h_o
$\theta(\beta)$	defined as $(a_o/a_N)^{4/3}$
λ	defined as H/d
λ_1, λ_2	parameters defined in eq 4 and 5
μ	viscosity, ratio of angular velocity (Ω_2/Ω_1)
υ	kinematic viscosity
ϱ	density
τ_w	shear stress
ϕ	defined as $(\beta/2)(T^*)_o'$
Φ	defined as $k\Delta T/\varrho L$
$\psi(\beta)$	defined as a_o/a_N
Ω	angular velocity
ω	defined in eq 54

Subscripts

c	critical
i	ice
iv	inversion
m	melting
md	average diameter
mH	average height
max	maximum
o	initial, without melting, surface
p	plate
w	wall
∞	bulk
1, 2	lower and upper boundary, or inner and outer

Thermal Instability and Heat Transfer Characteristics in Water/Ice Systems

YIN-CHAO YEN

INTRODUCTION

The phenomenon of convection in a horizontal water layer formed by melting either from below or from above is of special interest because the system divides itself into two regions with an unstable zone lying under a stable layer. This is caused by the nonlinear temperature–density relations of water possessing a maximum density. Figure 1 schematically shows the temperature and density profiles of the water layer continuously formed by melting ice from below. It can be seen from curve *a* that the water layer is stably stratified as long as $T_1 < 4°C$ and it is unstable when $T_1 > 4°C$ (the upper boundary is maintained at phase transition temperature, i.e. $T_2 = 0°C$). It is distinctly shown that the water layer between the ice/water interface and the 4°C isotherm is always stable. However, the relative height (i.e. the ratio of z/H, where z is the distance from the warm plate to the place where ϱ_{max} exists and H is the total layer depth) of the unstable region increases as T_1 increases. Figure 2 is a simple inversion of Figure 1 and shows the case of ice melting from above. In this case T_1 is at the melting temperature (i.e. $T_1 = 0°C$) and $T_2 > 0°C$. In contrast to Figure 1, the relative height of the unstable layer decreases with increasing T_2. Therefore, for water with its maximum density near 4°C, even for a constant temperature gradient, the density profile is a nonlinear function of the vertical ordinate z.

These situations are quite different from the classical Rayleigh problem in which a constant temperature gradient and a linear temperature–density relation of the fluid are assumed. In the classical problem, a fluid layer of constant depth confined rigidly from top and bottom but of infinite horizontal dimensions is either cooled from above or heated from below, and convection occurs if the temperature gradient exceeds a certain critical value. The criterion is usually expressed in terms of a Rayleigh number with a critical value of ≈ 1708, which has been verified by Bénard (1900) who observed the regular cell structure for $Ra > 1708$. This classical problem has been studied intensively since the early works of Rayleigh (1916) and Jeffreys (1926). Chandrasekhar (1961) provides a comprehensive analysis and summary of these studies. The aim of this study is to review and analyze the stability problem due to the density anomaly of water and its effect on the heat transfer characteristics in ice/water systems due to the evolution of the interfacial velocity that results from the density difference between ice and water.

ANALYTICAL STUDIES ON THE ONSET OF CONVECTION IN A HORIZONTAL WATER LAYER

The influence of the density anomaly of water on the onset of convection has been reported by quite a few investigators. Veronis (1963) was first to investigate the phenomenon of

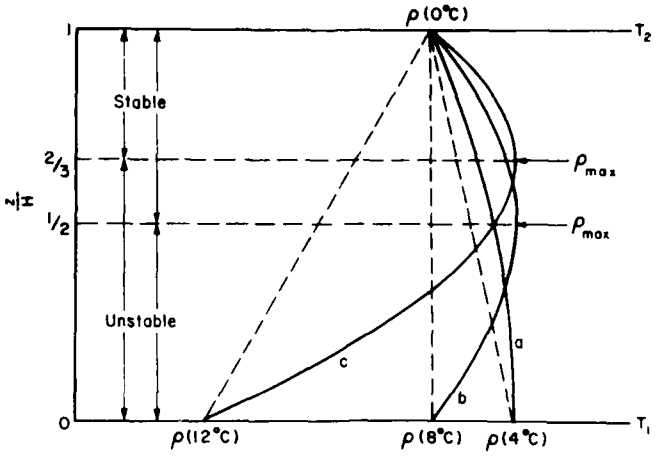

Figure 1. Schematic representation of the density profile in the conduction state for upper boundary $T_2 = 0°C$ *(equivalent to melting from below).*

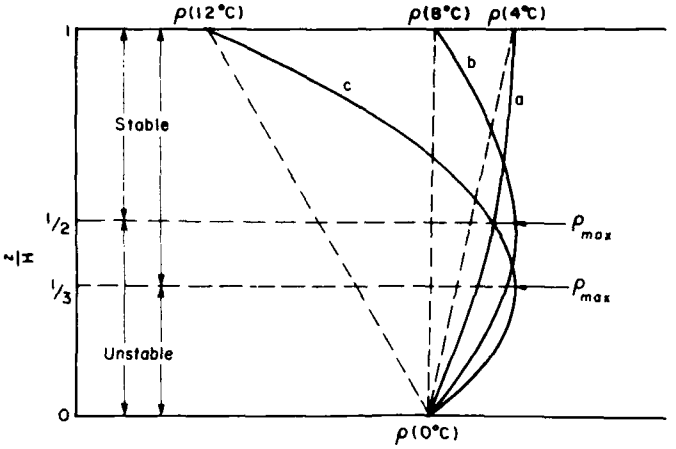

Figure 2. Schematic representation of the density profile in the conduction state for lower boundary $T_1 = 0°C$ *(equivalent to melting from above).*

penetrative convection. By representing the water density near 4°C with the quadratic expression

$$\varrho = \varrho_{max}[1-\gamma(T-T_{max})^2] \tag{1}$$

where ϱ_{max} is water density corresponding to T_{max} ($\simeq 3.97°C$) and $\gamma \simeq 7.68\times10^{-6}$ ($°C^{-2}$), and using linear stability theory, Veronis summarized the computed critical Rayleigh numbers Ra_c for both free (Table 1) and rigid (Table 2) boundaries. In both tables, λ is the ratio of the total layer depth H to the 4°C layer depth d in the conductive state (i.e. $\lambda = H/d$), a is the wave number, and Ra_c is the critical Rayleigh number. In Table 2, μ is defined as the ratio of the rotation rates of the outer to inner cylinder [$(1-\mu) \equiv \lambda$], Ta_c is the critical Taylor number. The values of a^2/λ^2 can be compared with values of $a^2/(1-\mu)^2\pi^2$ and $Ra_c/2\lambda^4\pi^4$ with $Ta_c/2(1-\mu)^4\pi^4$. There is of course a quantitative difference between the results of the two cases be-

Table 1. Critical Rayleigh numbers and corresponding wave numbers for various values of λ in rigid-free boundary problem (after Veronis 1963).

λ	a^2	Ra_c/π^4	a^2/λ^2	$Rac/2\lambda^4\pi^4$
0	0.500	6.75	—	—
1.0	0.500	13.43	0.5	6.75
1.2	0.505	16.69	0.351	4.03
1.4	0.519	21.92	0.265	2.81
1.6	0.535	31.37	0.209	2.40
1.8	0.630	50.86	0.194	2.42
1.9	0.750	67.07	0.205	2.58
2.0	0.930	87.18	0.233	2.73
2.5	1.64	222.2	0.262	2.84
3.0	2.29	547.9	0.254	2.83
3.5	3.10	854.7	0.253	2.84

Table 2. Critical Rayleigh numbers and corresponding wave numbers for various values of λ in rigid-rigid boundaries (after Veronis 1963).

$(1-\mu)\equiv\lambda$	a	Ta_c	$a^2/(1-\mu)^2\pi^2$	$Ta_c/2(1-\mu)^4\pi^4$
0	3.12	1.708×10^3	—	—
1	3.12	3.390×10^3	0.986	17.40
1.25	3.13	4.462×10^3	0.635	9.383
1.50	3.20	6.417×10^3	0.461	6.506
1.6	3.24	7.688×10^3	0.415	6.022
1.8	3.49	1.182×10^4	0.386	5.779
1.9	3.70	1.494×10^4	0.384	5.885
2.0	4.00	1.868×10^4	0.405	5.993
2.5	5.06	5.619×10^4	0.415	6.069
3.0	6.10	9.558×10^4	0.419	6.057
3.5	7.10	1.771×10^5	0.417	6.058

cause of the different boundary conditions, but it can be observed that the qualitative behavior is the same in both cases. In both tables, the unstable layer height d is used in defining the Rayleigh number. For the specific cases of $T_2 = 4$°C and 8 °C, i.e. $\lambda = 1$ and 2, Veronis reported Ra_c values of $13.43\pi^4$ and $87.18\pi^4$ respectively. These tabulated values of Ra_c clearly demonstrate that the onset of convection is dependent on the thermal boundary conditions imposed.

Sun et al. (1969) extended this work by adding a cubic term to the temperature-density relation

$$\varrho \approx \varrho_{max}[1-\gamma_1(T-T_{max})^2-\gamma_2(T-T_{max})^3] \tag{2}$$

that is valid up to 30°C. Following a procedure commonly employed in linear stability analysis, a modified Rayleigh number,

$$\mathrm{Ra} = \frac{2\gamma_1 A g(\Delta T)^2 H^3\left(1+\frac{3}{2}\frac{\gamma_2}{\gamma_1}A\Delta T\right)}{\alpha\upsilon}, \tag{3}$$

is derived in which $A = (T_1-T_{max})/(T_1-T_2)$, H is the total melt layer depth, and ΔT is the overall temperature difference (i.e. $\Delta T = T_1-T_2$). They found the Ra values were functions of two parameters defined as follows:

$$\lambda_1 = \left(-\frac{1}{A}\right)\frac{1+3\frac{\gamma_2}{\gamma_1}A\Delta T}{1+\frac{3}{2}\frac{\gamma_2}{\gamma_1}A\Delta T} \tag{4}$$

and

$$\lambda_1 = \left(-\frac{1}{A^2}\right)\frac{\frac{3}{2}\frac{\gamma_2}{\gamma_1}A\Delta T}{1+\frac{3}{2}\frac{\gamma_2}{\gamma_1}A\Delta T} \tag{5}$$

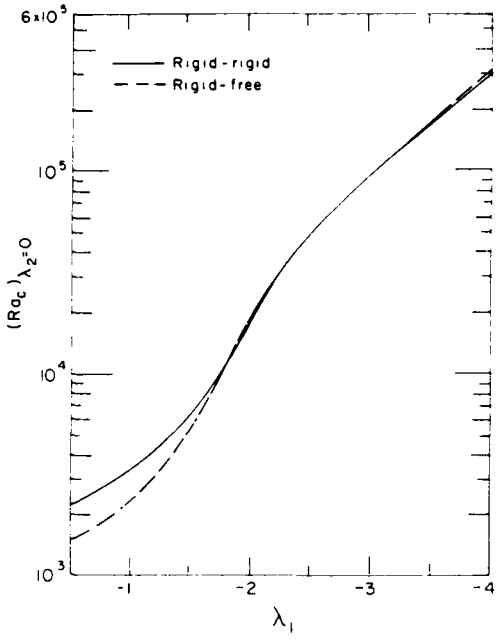

Figure 3. $(Ra_c)_{\lambda_2=0}$ as a function of λ_1 (after Sun et al. 1969).

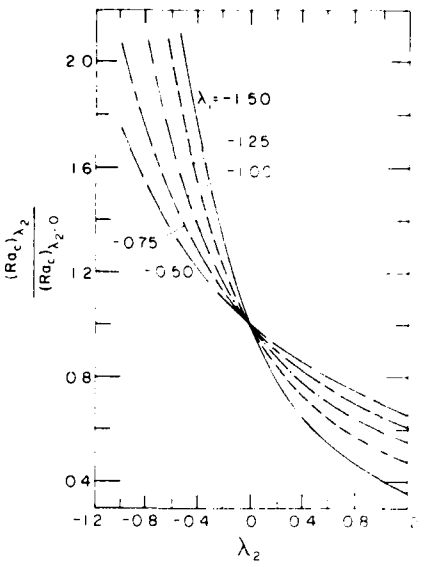

Figure 4. $\frac{(Ra_c)_{\lambda_2}}{(Ra_c)_{\lambda_2=0}}$ vs λ_2 with λ_1 as a parameter for the rigid-free case (after Sun et al. 1969).

Ra_c values are computed for ranges $-4.25 < \lambda_1 < -0.5$ and $-1.4 < \lambda_2 < 1.6$. Numerical values of $(Ra_c)\lambda_2 = 0$ (i.e. for the case of parabolic temperature-density relation, $\gamma_2 = 0$, and $\lambda_1 = -1/A$ as a function of λ_1 were reported and shown in Figure 3 for both rigid-free and rigid-rigid boundaries. The Ra_c values for cubic and parabolic temperature-density relations were expressed in a ratio as $(Ra_c)_{\lambda_2}/(Ra_c)_{\lambda_2} = 0$ and was shown vs λ_2 using λ_1 as the parameter for rigid-free (Fig. 4) and rigid-rigid boundary conditions (Fig. 5). These results are valid as along as the melt layer contains a density extremum within the boundaries.

Merker et al. (1979) studied this same problem with the representation of the temperature-density of water approximated by three different polynomials having 2, 3, and 5 terms. Linear stability analysis was used and the resulting perturbation equations were solved with the aid of Galerkin's method. Figure 6 shows the general diagram of stability for fluids having a density extremum in which the values of β_1 and β_2 are the

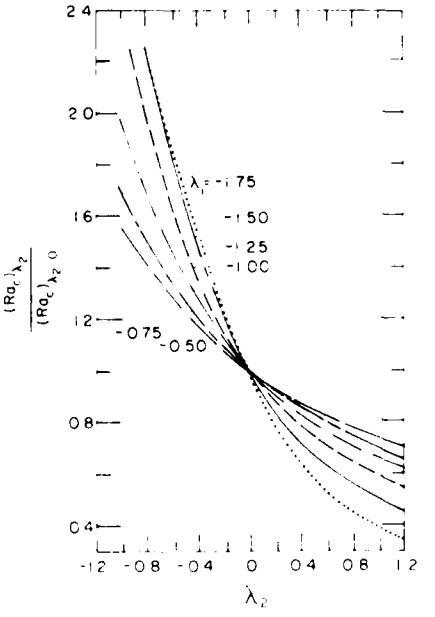

Figure 5. $\frac{(Ra_c)_{\lambda_2}}{(Ra_c)_{\lambda_2=0}}$ vs λ_2 with λ_1 as a parameter for the rigid-rigid case (after Sun et al. 1969).

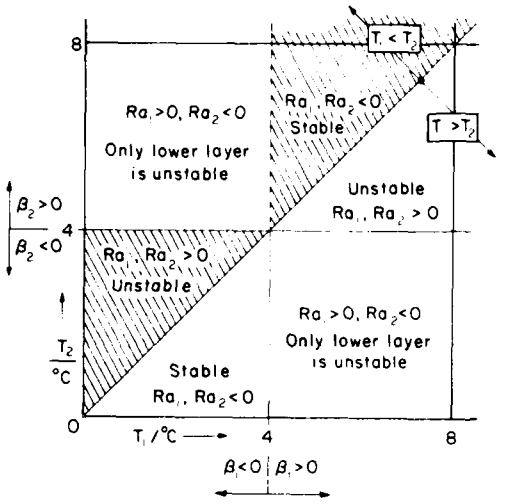

Figure 6. Principal stability diagram (after Merker et al. 1979).

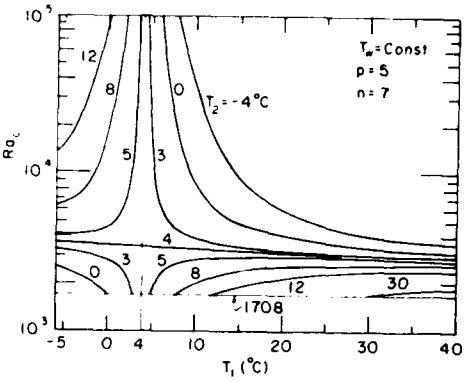

Figure 7. Critical Rayleigh number Ra_c as a function of T_1 with T_2 as a parameter for T_w (wall temperature) = constant (after Merker et al. 1979).

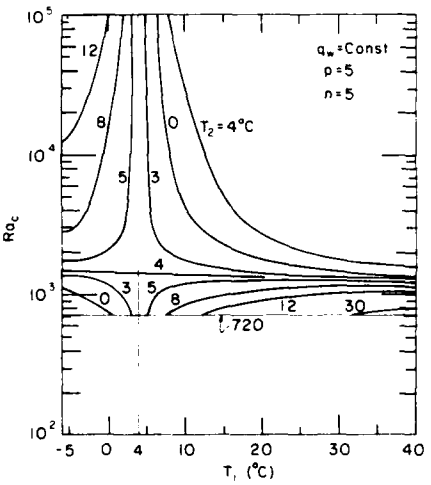

Figure 8. Critical Rayleigh number Ra_c as a function of T_1 with T_2 as a parameter for q_w = constant (constant wall flux) (after Merker et al. 1979).

coefficients of thermal expansion evaluated at T_1 and T_2 respectively, and the values of Ra_1 and Ra_2 are the corresponding Rayleigh numbers, defined as $Ra = gH^3\beta\Delta T/\alpha\upsilon$ in which H is the total layer depth, $\Delta T = T_1 - T_2$, g is the gravitational acceleration, α is the thermal diffusivity, and υ is the kinematic viscosity. Since Ra_1 is always defined as positive if the layer is unstably stratified, whereas Ra_2 changes sign, Ra_1 was used by Merker et al. (1979) to describe the layer stability. Figure 7 shows the critical Rayleigh number variation with T_1 in the case of constant wall temperature (i.e. T_w = constant) with the density-temperature relation represented by a polynomial of order $p = 5$ and $n = 7$ (number of Galerkin terms). Figure 8 shows the case of constant wall heat flux density (i.e. q_w = constant). In both figures, it can be noted that in the region below isotherm $T_2 = 4$°C, the water layer has a density profile with no maximum value, i.e. the layer is completely unstably stratified. However, the nonlinearity of the density profile is slight and the effect on the critical Rayleigh number is not large. Ra_c is in the range of 1708 to $\approx$ 3600 for T_w = constant and 720 to $\approx$ 1600 for q_w = constant. On the other hand, for the region above isotherm $T_2 = 4$°C, the layer has a density profile containing a maximum value between the two boundaries and the layer is only partially unstably stratified. The nonlinearity of the density profile is strong and the effect on Ra_c is great. The Ra_c values are significantly larger than those obtained from the classical problem. For constant wall temperature and rigid boundary conditions, this work should be comparable to the work of Sun et al.

(1969) in which a cubic density-temperature relation was used and the entire layer depth (as in this work) was used in defining the critical Rayleigh number.

EXPERIMENTAL STUDIES OF THE ONSET OF CONVECTION IN A CIRCULAR HORIZONTAL MELT LAYER

The first experimental study that focused solely on determining the onset of convection in a water layer formed by melting ice was reported by Yen (1968). In a study of the effect of buoyancy on the melting and freezing process, Boger and Westwater (1967) claimed the critical Rayleigh number, Ra_c($Ra = gH^3\Delta T\beta/\alpha\upsilon$) in a system involving phase change and density inversion, was around 1700, nearly identical to the value reported by Globe and Dropkin (1959) and Schmidt and Silveston (1959), who heated the horizontal layers of water from below but did not test in the region of the density inversion. However, to have $Ra_c \approx 1700$ as in the classical case of normal fluid (i.e. density is a monotonic function of temperature), proper values of H, β, ΔT, α, and υ had to have been used depending on the direction of melting (upward or downward) and the thermal boundary conditions. If the ice is at the top (i.e. melting from below), $\Delta T = T_i - 4°C$, H is the total layer depth, β is evaluated at T_i, and the other properties of α and υ are evaluated at $\frac{1}{2}(T_i + 4°C)$. If the ice is at the bottom (i.e. melting from above), they proposed using $\Delta T = 4°C$, H is the portion of water layer depth and was evaluated by equating the heat transported through the convective layer to the heat conducted through the ice, i.e. $H = -4d_i k_e/k_i T_i$, in which d_i, k_i, and T_i are thickness, thermal conductivity, and temperature (maintained at the end of the sample of ice), k_e is the effective thermal conductivity of water of the convective layer, β is evaluated at 0°C, and α and υ are evaluated at the mean temperature of the buoyant region, i.e. 2°C. In Yen's work, a rather large, cylindrical, bubble-free ice sample was used (12.7 cm in diameter and 25 cm high) and at the beginning of the experiment there was only one solid phase. A constant temperature boundary was applied at the lower end, which resulted in melting from below. Because of the rapid transition of the melt layer from the conductive to the convective state, it restrained the upper limit of the temperature that could be imposed. For T_i ranging from 7.72 to 25.2°C and using the criteria recommended by Boger and Westwater (1967) in evaluating Ra_c, he found on the contrary that the Ra_c values were a strong function of T_i and can be represented by

$$Ra_c = 14{,}200 \exp(-6.64 \times 10^{-2} T_i). \quad (6)$$

The initial temperature of ice T_0 was found to have had no significant effect on the Ra_c values. Figure 9 strongly shows the variation of Ra_c with the lower boundary temperature.

It should be emphasized that the study of the melt layer is quite distinct from the classical problem of a horizontal layer of fluid of invariant depth. For a water layer formed by melting, the layer depth not only grows with time but simultaneous addition of water is necessary to make up volume shrinkage due to phase transition (an intricate device has to be found to conduct studies of this na-

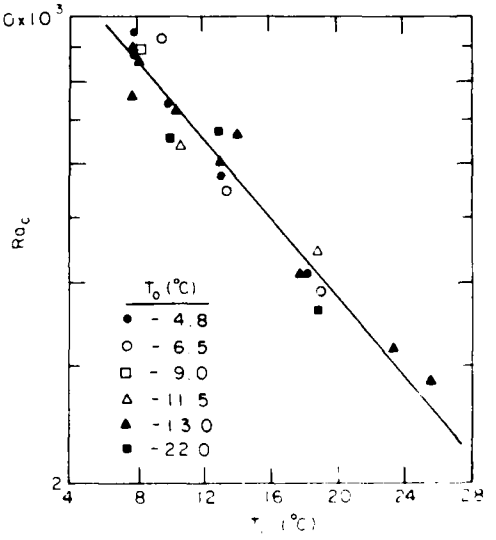

Figure 9. Ra_c as a function of T_i (after Yen 1968).

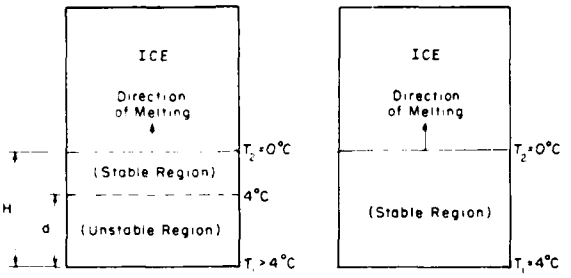

a. Melting from below.

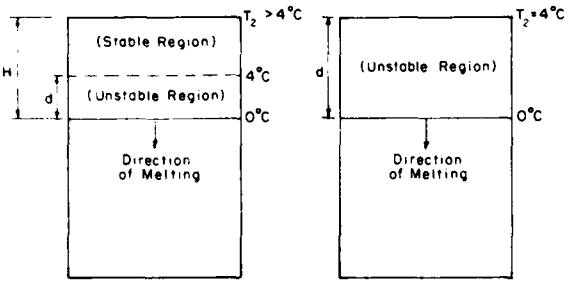

b. Melting from above.

Figure 10. Schematic representation of the interdependence of stable and unstable regions with the thermal boundary conditions.

ture). The water layer can be formed either by melting from below or above. For the case of melting from below (i.e. $T_1 > 4°C$, $T_2 = 0°C$; for the special case of $T_1 = 4°C$, the entire water layer will always be stable), an unstably stratified region will extend from the lower boundary up to the 4°C isotherm and a stable region above the 4°C isotherm will extend to the upper boundary (the water/ice interface). On the other hand, for the case of melting from above (for $T_2 > 4°C$, $T_1 = 0°C$), there will be a stable layer adjacent to the upper boundary and an unstable region between the 4°C isotherm and the water/ice interface, while for $T_2 = 4°C$, the entire melt layer will be unstably stratified. Figure 10 shows the interdependence of the stable and unstable regions with the thermal boundary conditions. In a follow-up study on melting from below and above, Yen and Galea (1959) reported that the critical layer depth H_c (at which the heat transfer mode changes from conduction to convection) could be determined either by locating the inflection point on the melting front vs time or by locating the sudden jump of the temperature gradient in the stable region. Figure 11 shows the variation of the temperature gradient as a function of time and the upper boundary temperature (cases of melting from above). It can be seen that the higher the upper boundary temperature, the more shallow the temperature gradient jump at the onset of convection. Figure 12 compares the Ra_c values for melting from below and from above. Experimental Ra_c values were evaluated using appropriate values of critical layer depth H_c: A = (I I_{max}) I . ΔT I for melting from below and $A = t_{max}/T_2$, $\Delta T = -T_2$ for melting from above. Theoretical Ra_c values were determined from a graph developed by Sun et al. (1969) (Fig. 5 in this paper) after evaluating parameters λ_1 and λ_2 from eq 4 and 5. Figure 13 demonstrates another way of comparing Ra_c values using T_1 or T_2 explicitly as a variable. This figure covered I from 7.72 to 25.2 °C and T_2 from 6.3 to 13.09°C. The corresponding ranges of and are from 1.970 to 0.830 and λ_2 from -0.311 to 0.390 for melting from below, and from 3.444 to 1.618 and λ_2 from 0.112 to 0.508 for melting from above.

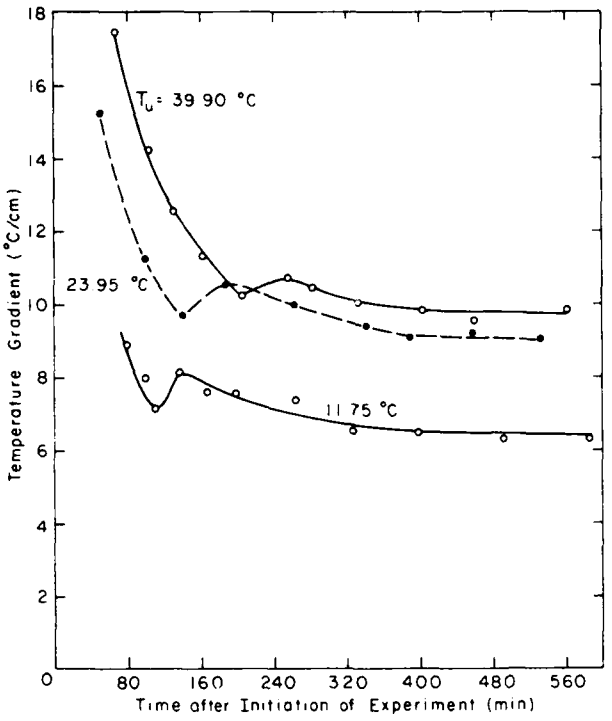

Figure 11. Variation of temperature gradient in the stable region of the water layer (near the upper boundary).

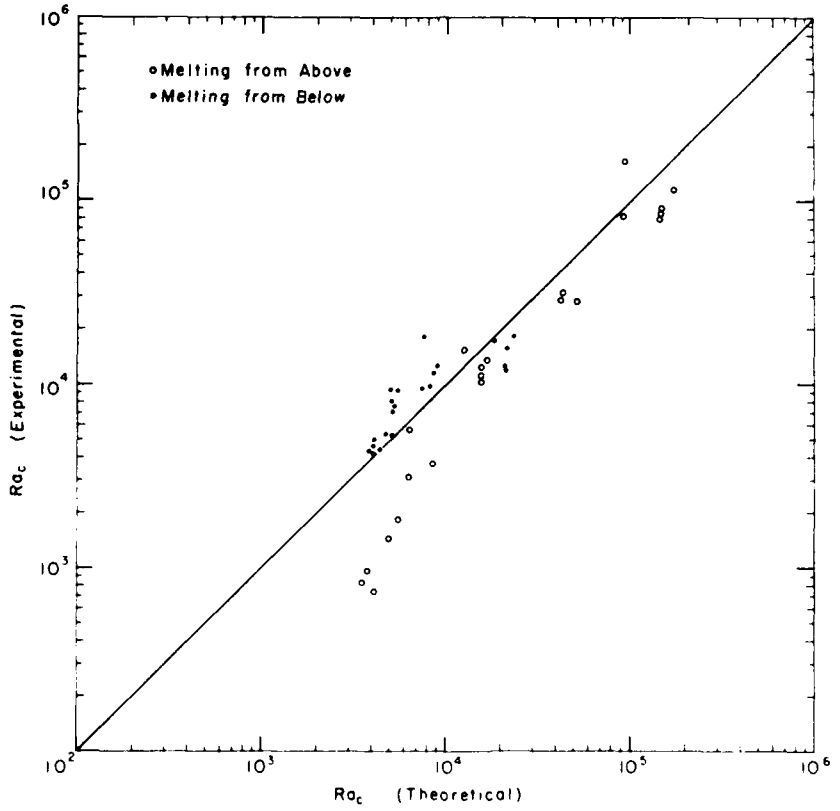

Figure 12. Comparison of experimental and theoretical Ra_c (after Yen and Galea 1969).

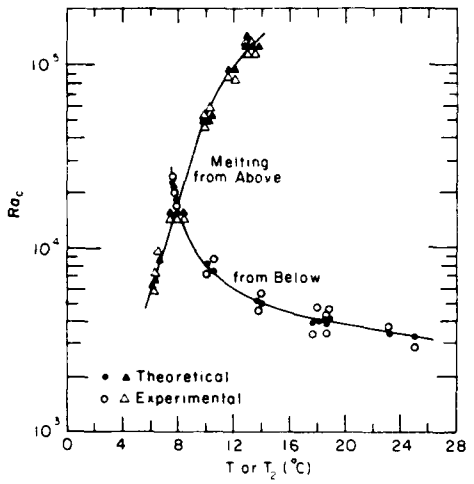

Figure 13. Comparison of experimental and theoretical Ra_c using T_1 or T_2 as the variable (after Sun et al. 1969).

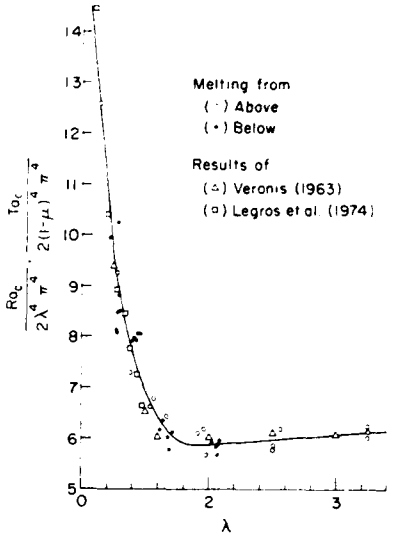

Figure 14. Comparison of $Ta_c/[2(1-\mu)^4\pi^4]$ and $Ra_c/(2\lambda^4\pi^4)$ vs λ (after Yen 1980).

The experimental results of Yen (1968) and Yen and Galea (1969) were also compared with the analytical work of Veronis (1963) and the experimental work of Legros et al. (1974). Veronis considered the case equivalent to melting from above while Legros et al. studied the case equivalent to melting from below. In both cases, however, the layer was invariant, while in the studies of Yen (1968) and Yen and Galea (1969) the water layer was formed (initially at zero depth) continuously as a resultant of phase transition. Veronis' results were plotted in terms of $Ta_c/2(1-\mu)^4\pi^4$ vs λ in which Ta_c is the critical Taylor number. The work of Legros et al. was expressed in terms of $Ra_c/2\lambda^4\pi^4$, in which Ra is defined as

$$Ra = g\gamma(\Delta T)^2 d_c^2/\alpha\upsilon$$

where γ is a temperature coefficient as defined in eq 1, ΔT is the temperature difference across the unstable layer and in the cases of melting from above and below, $\Delta T = 4°C$ and $T_i - 4°C$ respectively [due to the presence of $(\Delta T)^2$ in the definition of Ra, this comparison should be valid for both cases of melting]. The values d_c are evaluated as follows: For melting from above $d_c = -(4/T_2)H_c$, and for melting from below $d_c = [(T_i-4)/T_i]\,H_c$. Figure 14 shows a remarkable agreement among these studies.

Some unique features were observed in the studies reported by Yen (1968) and Yen and Galea (1969) during the formation and continuous deepening of the water layer. Prior to the onset of convection, the water/ice interface remains a planar surface and the prevailing heat transfer mode is conduction. Cells start to form as soon as the Ra_c value is attained. At the very beginning stage, these cells possess regular patterns and are hemispherical and higher in the center. They have a circular cross-section, differing from the well-known hexagonal Bénard cells, and are distributed evenly over the entire water/ice interface. Figure 15a shows schematically the interface morphology observed shortly after the onset of convection in the case of melting from below. It is interesting to note that in the case of melting from above, a stable region would form over the unstable region adjacent to the interface as soon as the melted layer was formed. The interface (see Fig. 15b), in contrast to the case of melting from below, is covered with a series of circular concentric ridges equally spaced from each other.

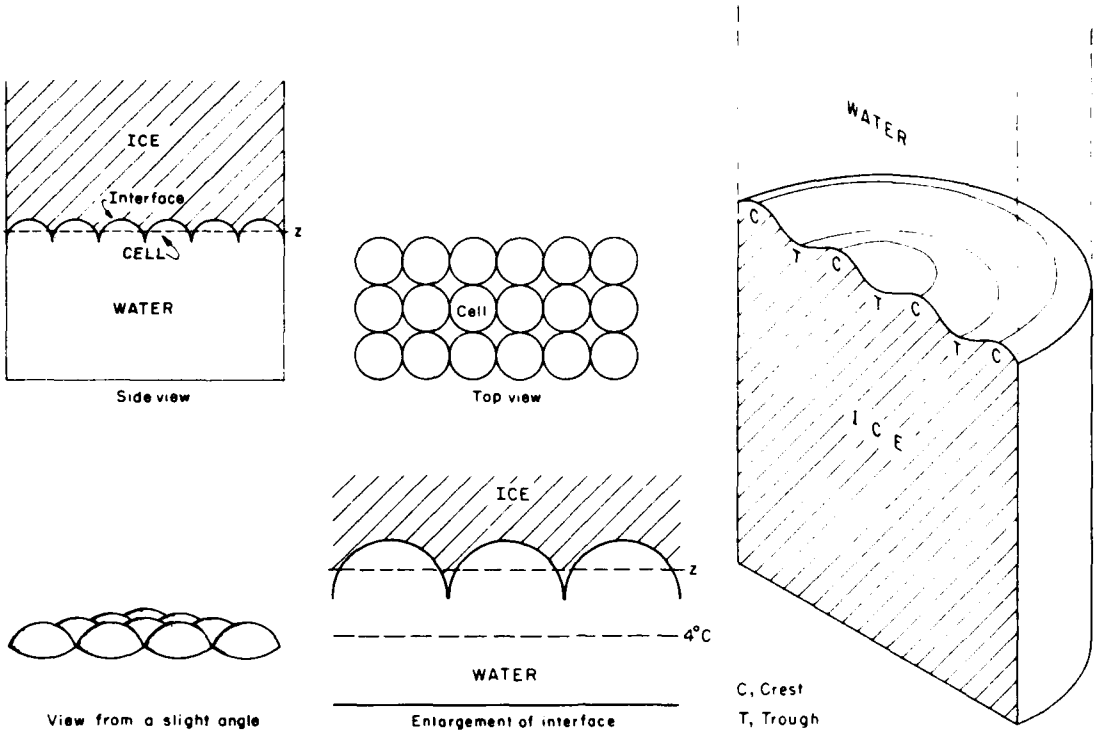

a. Melting from below. *b. Melting from above.*

Figure 15. Schematic of water/ice interface shortly after onset of convection (after Yen and Galea 1969).

The height between crest and trough increases with time and it can reach a value as large as 5.0 mm. However, this pattern was replaced by that of small inverted hemispherical cells that gradually enlarged and finally formed an irregular and unsymmetrical interface as the melting progressed (as in the case of melting from below).

TEMPERATURE STRUCTURE AND HEAT TRANSFER

In a horizontal layer

Townsend (1964) was the first to make a detailed study of the temperature structure and natural convective heat transfer in water over an ice surface. The experimental tank consisted of a 30- × 30-cm bottom made of Dural 0.95 cm thick with sides made of Perspex of the same thickness. Distilled water filled the tank to a depth of 15 cm, and the tank bottom was cooled by a shallow dish filled with liquid nitrogen (not in direct contact with the bottom, however; it should be noted that the purpose of bottom cooling was only to maintain the lower boundary at 0°C). The free water surface temperature was maintained electrically through another Dural plate suspended about 5 mm above. The most striking feature of the steady temperature distribution was the creation of a region of constant mean temperature. Townsend indicated that, after establishing a constant mean temperature region, the only observed change was the upward extension of its boundary. Figure 16 shows the temperature distributions during the approach to equilibrium. Figure 17a shows the equilibrium distribution of the mean temperature. It can be seen that the constant temperature region has a mean temperature of 3.2°C, significantly below the temperature of maximum density (i.e. ≈ 4°C).

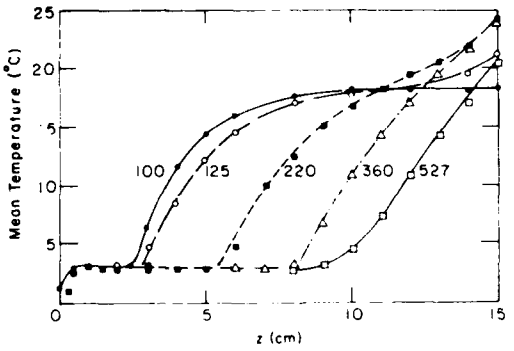

Figure 16. Temperature distribution during the approach to equilibrium. The numbers by the curves are the elapsed times in minutes from the start of cooling (after Townsend 1964).

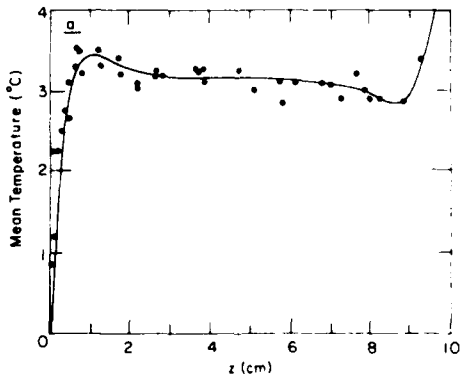

a. Unstable and "constant temperature" regions.

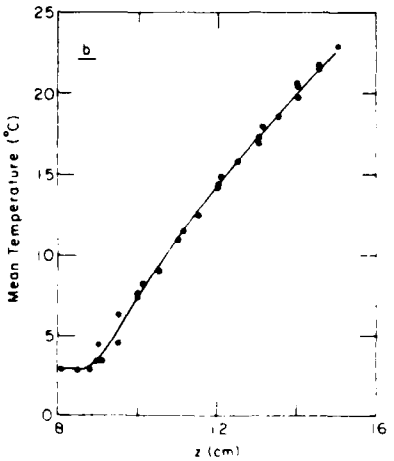

b. Stable and disturbed regions (note scatter of points for temperatures near 6 °C, indicating unusually large fluctuations).

Figure 17. Mean temperature distribution for thermal equilibrium corrected to a surface temperature of 23 °C (after Townsend 1964).

Townsend also noted the peculiarities of "overshoot" regions at each end where the gradient of the mean temperature changes sign (Fig. 17a). The mean temperature increases with height and reaches 3.6°C before decreasing to 3.2°C; at the upper limit of the region it falls to 2.9°C before increasing rapidly in the stable region above. The upper overshoot was postulated to be a consequence of the slowing down of the lower parts of rising columns of cold water as their tops enter the stable layer. However, Townsend stated that the lower overshoot cannot be interpreted in a similar manner, as descending columns of hotter water are not observed, and he indicated this may be attributed to the subsidence of water with a temperature between 3.2 to 4°C. Townsend also noted large fluctuations of temperature just within the region of stable stratification but they fell off very rapidly with height and were very small if the local temperature exceeded 10°C (Fig. 17b).

Townsend evaluated the downward heat flux q (i.e. the heat extracted through the tank bottom) by fixing $z = z_r$ as a reference plane in the stable region and assuming horizontal homogeneity as follows:

$$q = -\varrho c_p \frac{d}{dt} \int_0^{z_r} (T - T_r) dz + k\left(\frac{\partial t}{\partial z}\right)_{z=z_r} \tag{7}$$

where the first term on the right represents the rate of change of heat content below fixed plane z_r, T is the local mean temperature, T_r is the reference temperature (taken to be 3.2°C), ϱ, c_p, and k are the density, heat capacity, and thermal conductivity of the water, and z is the distance measured vertically upward from the ice surface.

With the measurement of T both in the stable and unstable regions as a function of time, the two terms on the right of eq 7 can be evaluated. The heat flux was reported to be from 34 mW/cm^{-2} in the beginning, decreasing to about 26 mW cm^{-2} as the temperature distribution approaches equilibrium. He attributed this reduction to heat intake through the side walls of the test tank as the thick, cold, constant-temperature region formed. However, since there were no changes in temperature distribution and the pattern of convection, he concluded that the equilibrium heat flux in a horizontally homogeneous system would be close to 34 mW cm^{-2}. Using this flux, Townsend derived the following expression:

$$Q = \frac{q}{\varrho c_p} = 0.156(\Delta T)^{5/3} (\gamma \beta g)^{1/3} (\alpha/\upsilon)^{1/3} \tag{8}$$

in which ΔT is the temperature difference between the tank bottom and the temperature of maximum density T_{max} = 3.98°C and γ is defined in eq 1. Equation 8 is the dimensionally analogous form for the heat loss from a smooth heated plane involving fluids with linear expansion given by

$$Q = 0.193(\Delta T)^{4/3} (\alpha \beta g)^{1/3} (\alpha/\upsilon)^{1/3} \tag{9}$$

in which ΔT is the temperature difference between the surface and far above the plane.

Myrup et al. (1970) also studied this convection problem over ice, which they found has great value in understanding and modeling geophysical and astrophysical convection systems. Their experimental set-up was similar to Townsend's. The water was initially at room temperature and the tank bottom was maintained slightly higher than 0°C by a water and ice bath beneath it. The top of the tank was covered with an aluminum plate in direct contact with the water surface that was conditioned to equilibrium with the room air. They made extensive measurements on mean temperature profiles as well as temperature fluctuations at every level. Temperature profiles similar to those of Townsend were reported. Figure 18 shows a reproduction of the temperature record at a single height of 2.8 cm above the lower

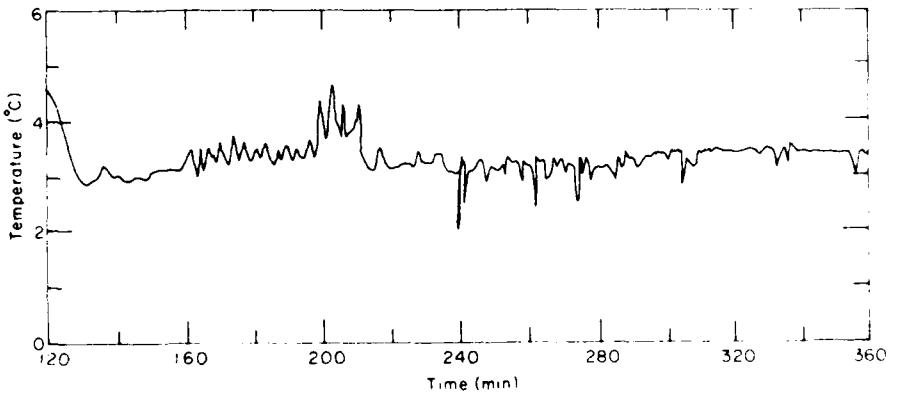

Figure 18. Temperature at 2.8 cm above the lower boundary maintained near 0°C (after Myrup et al. 1970).

plate (bottom). It is evident that distinctly different kinds of temperature fluctuations occurred. At about 160 to 220 minutes after the beginning of the experiment there were some sort of periodic warm fluctuations, some of which were warmer than 4°C. This phenomenon was attributed to the effects of gravity waves bobbing up and down in the stable layer just above the convective layer. From 220 minutes on, the temperature fluctuations distinctly changed. The irregular cold deviations are due to penetrations by convective plumes of the buoyant cold fluid rising from the lower boundary layer. Photographs delineated the formation and subsequent development of three distinct layers. The boundary layer, nearest the lower plate, is occupied by the densest concentration of the dye; the dark upper portion is the fluid warmer than 4°C into which the dye-laden convective currents have not penetrated, and in between is the convective layer. Myrup et al. (1970) made no attempt in their study to evaluate the heat fluxes.

In a circular horizontal melt layer

Along with the study of the determination of the onset of convection in the melt layer, the mean temperature of the growing melt layer was measured intermittently (Yen 1968, Yen and Galea 1969). The ice/water system in these studies was drastically different from those in the works reported by Townsend (1964) and Myrup et al. (1970) in that only solid ice was present at the onset of the experiment. The depth of the melt layer started from zero and deepened continuously as the melting progressed either from above or below. Thermistors with a 0.02-s response time were used to measure intermittently the temperature profile of the growing layer. To minimize possible disturbance of the temperature field when the thermistors were inserted, they were installed at different radii and distributed over the circular area. Typical mean temperature profiles are shown in Figure 19, for melting from below, and in the following figure, for melting from above. Each data point represents four thermistor readings from the same layer depth. It is noted that for both melting cases the thermistor readings contained a random component associated with the fluctuating temperature fields in the convection region, demonstrating that the convective motion was unsteady. Figure 19a shows the temperature profile just before the onset of convection for T_i at 4.02, 6.65, 7.46, 8.11, and 9.84°C respectively, with initial temperature T_o at -11.5°C. It clearly shows that, for 4.02°C at 418 minutes after the beginning of the experiment, the temperature profile remains linear as expected (theoretically the melt layer will remain stable indefinitely as long as $T_i \approx 4$°C). However, for T_i at 9.84°C, the convection was about to commence barely 36 minutes after the experiment started. This demonstrated strongly the dependence of the layer stability on the imposed T_i. At the onset of convection (Fig. 19b), the temperature curves are all deviated upward from the linear. In all these figures, the number by each curve is the time elapsed from the initiation of the experiment; the times chosen were nearly equal to each other to show the significance of T_i affecting the onset, and implicitly the intensity, of the convective mixing of the unstable region. Figure 19c shows the pseudo-steady-state temperature distribution of the melt layer; it consisted of a nearly constant temperature zone, but this constant temperature was noted to be dependent on the T_i imposed, i.e. the higher the value of T_i, the higher the temperature of the constant temperature zone. The four thermistor readings at each level exhibited considerable fluctuations, especially at the intersection between the convective and the upper conductive layer adjacent to the water/ice interface.

Figure 20 shows some typical mean temperature profiles of the melt layer formed by melting from above. Contrary to the previous cases, the layer is most stable when T_2 is the highest (because the driving force to create the convective motion merely results from the density differences between 0° and ≈4°C). Figure 20a shows the mean temperature profiles just before convective motion starts for T_2 ranging from 11.92°C to as high as 39.75°C. It can be observed that the melt layer became progressively more stable as T_2 increased. Figure 20b dis-

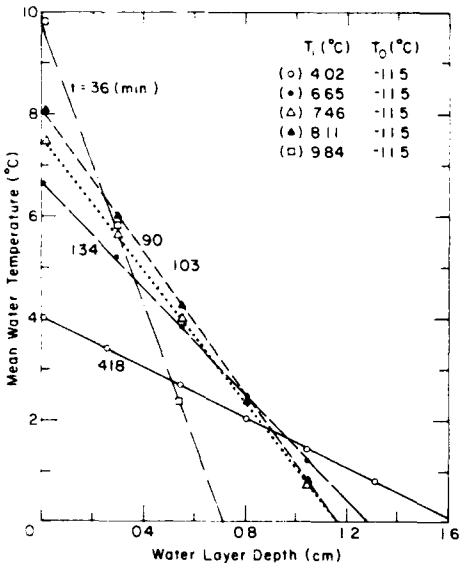

a. Before onset of convection.

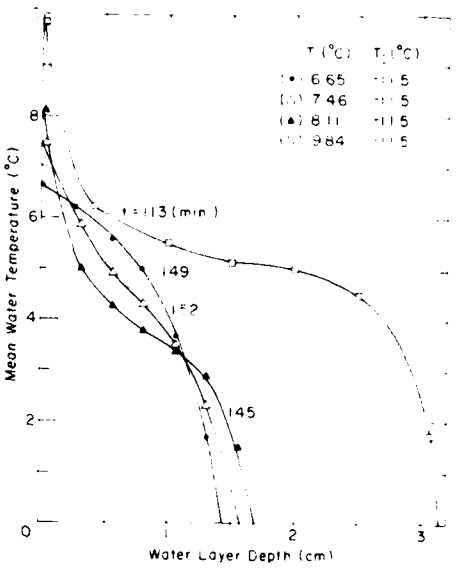

b. Development of the convective layer.

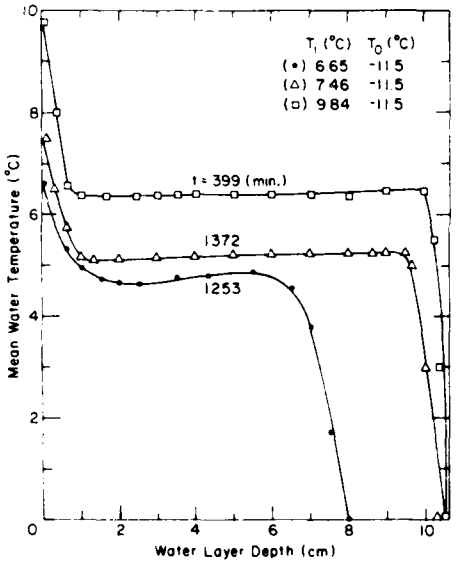

c. Pseudosteady state.

Figure 19. Mean temperature profiles for melting from below (after Yen 1984).

tinctly shows that (after almost the same time span), for $T_2 = 39.75°C$ and at $t = 238$ min, the temperature is just beginning to deviate from the linear distribution, but on the other hand, for $T_2 = 11.95°C$ and at $t = 256$ min, a constant temperature region is already well developed. Figure 20c shows clearly the establishment of the well-developed constant temperature zone as shown in Figure 19c but, contrary to the case of melting from below, the constant temperature zone is $\approx 3.2°C$ regardless of what value of T_2 was imposed on the upper boundary. Slight temperature reversals can be observed in Figures 19c and 20c. Overshoots were noted in all temperature traverses (regardless of whether the melting was from above or below) in the pseudosteady conditions, substantiating the findings of Townsend (1964).

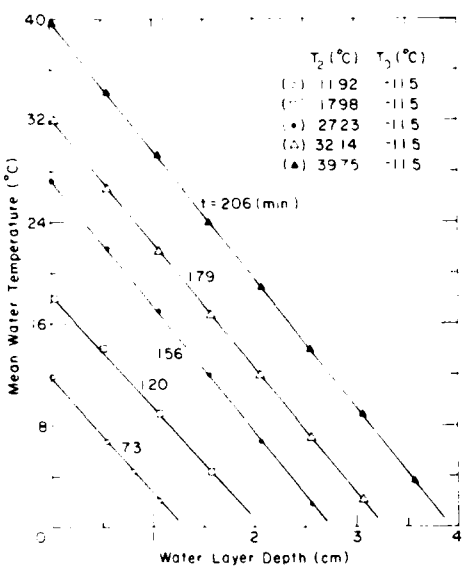

a. Before onset of convection.

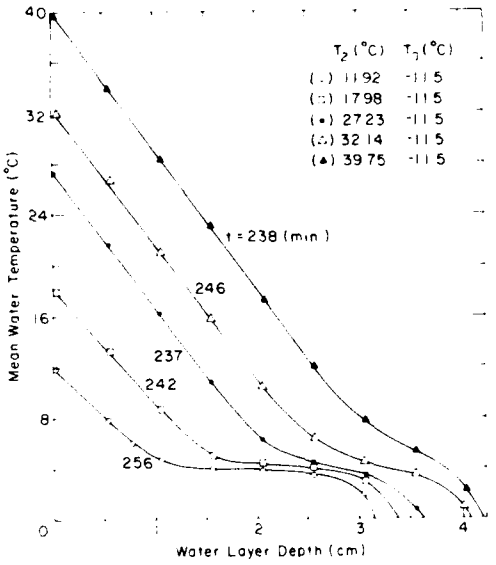

b. Development of the convective layer.

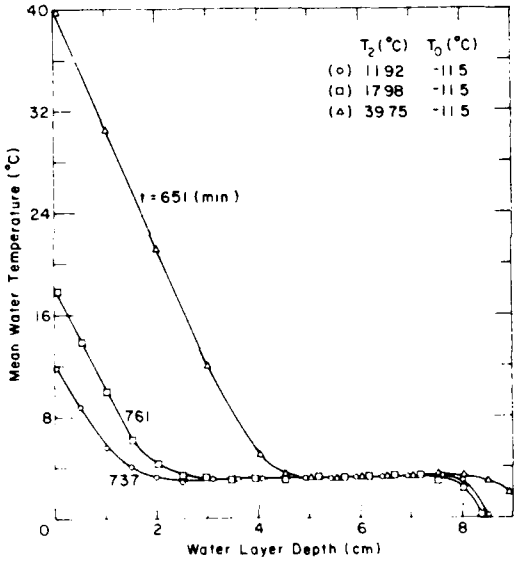

c. Pseudosteady state.

Figure 20. Mean temperature profiles for melting from above (after Yen 1984).

Typical mean temperature data have been made dimensionless by use of the molecular scales of velocity, length, and temperature for convection in water over ice given by Townsend (1964):

$$\omega_o = (\alpha\gamma g Q^2)^{1/5},\ Z_o = \alpha/\omega_o,\ \theta_o = Q/\omega_o \tag{10}$$

or the convection scale defined as

$$\omega_x = (\gamma g Z_x Q^2)^{1/4},\ Z_x,\ \theta_x = Q/\omega_x \tag{11}$$

in which the convection scale length Z_x is taken as the height of the convection layer as indicated by Adrian (1975). It is designated as the height at which the mean temperature reached 3.98°C.

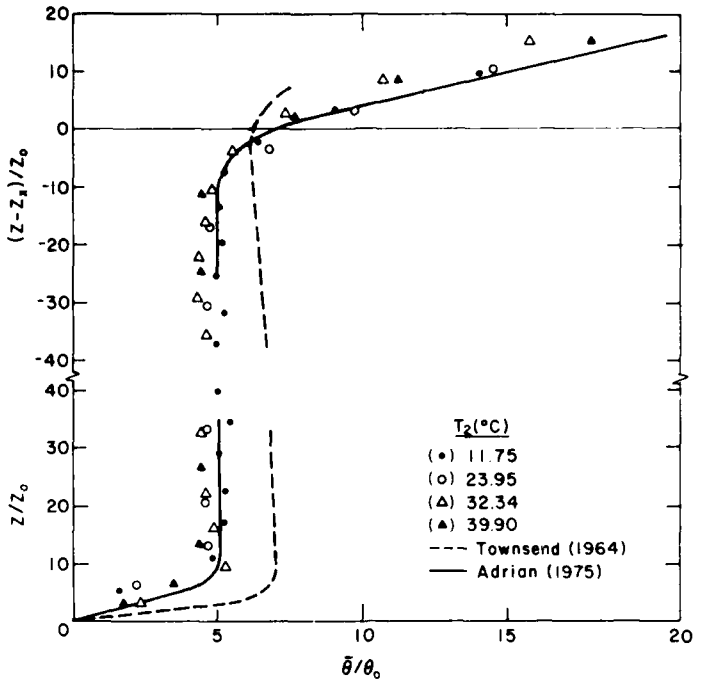

Figure 21. Nondimensional mean temperature profile for melting from above (after Yen 1980).

The molecular scales are based on the assumption that in certain regions of the flow the convection-layer depth is not dynamically significant, but molecular diffusion is important. Hence, the molecular scales are expected to be appropriate in the boundary layer regions such as the conduction layer and the interfacial layer. On the other hand the convection scales are intended to apply in the core of the convection layer where the length scale of the convection motion is on the order of the layer depth. Figure 21 shows the typical nondimensional mean temperature profile for the case of melting from above, including the works of Townsend (1964) and Adrian (1975) on convection of water over ice (a thin layer at maximum). It should be pointed out that in Townsend's and Adrian's work, the water layer did not result from melting; instead an invariant and rather deep water layer ($\approx$ 15 cm) was used. Adrian's results seem to agree remarkably well with Yen's (1984).

Figure 22 shows the nondimensional mean temperature profile for melting from below. The shape of the curve is the opposite of the curve shown in Figure 21. It should be pointed out that the temperature of the convection layer, indicated in Figure 19c as depending on the value of T_i, the nondimensional mean temperature—derived from the limited available data—fell more or less on a single curve as shown in Figure 21, with a somewhat higher ratio of θ/θ_o for the convection layer. The only experimental work closely related to the case of melting from below was conducted by Legros et al. (1974) for those experiments with an upper boundary less than 4°C. However, their work was aimed at determining the critical temperature difference across the layer, and no attempt was made to measure the temperature profile within the layer.

Yen (1980) also derived heat flux expressions for the melt layer formed by melting from both below and above. For experiments in which the melting rates were determined, the total upward or downward heat flux for melting from below or above was evaluated by

$$q = \varrho \frac{dz}{dt}[L + c_i(T_m - T_o)] + \frac{\varrho c_p}{2t}[z(t)(T + T_m)] - k_i \frac{dT_i}{dz}\bigg|_{z = H_c}. \qquad (12)$$

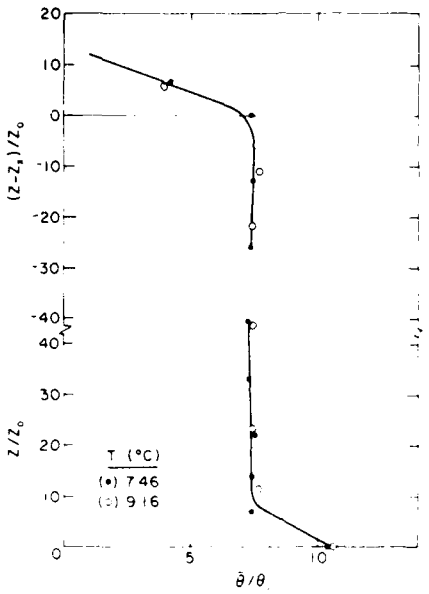

Figure 22. Nondimensional mean temperature profile for melting from below (after Yen 1980).

The term $(\varrho c_p/2t)[z(t)(T+T_m)]$ represents the mean sensible heat content variation of the entire layer of a depth $z(t)$. In the case of melting ice, $T_m = 0°C$ and T stands for either T_1 or T_2. The contribution of this term to the overall heat flux was found to be much more significant in the case of melting from above. For those experiments in which the mean layer temperature was measured as the melting progressed, the heat flux was approximated by

$$q = \frac{\Sigma \frac{k}{2}\left[\left(\frac{dT}{dz}\right)_2 + \left(\frac{dT}{dz}\right)_1\right](t_2-t_1)}{\Delta t} \qquad (13)$$

in which $(dT/dz)_2$ and $(dT/dz)_1$ are the mean temperature gradients at the stable region near the upper boundary for melting from above and the lower warm plate for melting from below. Subscripts 1 and 2 indicate the beginning and end of each period and Δt is the total time period. For calculating a value of q, at least a dozen or more of these periods (with varying durations) were used. The heat flux from above was found to be a weak function of T_2 and can be represented by

$$q = 177(T_2)^{0.303} \qquad (14)$$

with an average $q \simeq 374$ W/m². The above expression is valid for T_2 ranging from 11.75 to 39.9°C. For melting from below, Yen (1980) reported

$$q = -1900 + 315(T_1). \qquad (15)$$

For T_1 ranging from 7.7 to 25.5°C, the heat flux is found to be a linear function of T_1. Higher values of T_1, and thus higher temperatures in the convective zone, resulted in greater convective motion in the unstable region and consequently reduced the thickness of the stable layer adjacent to both the ice and the thermal boundary. The works of Townsend (1964) and Adrian (1975) are similar to the case of melting from above. However, in their investigations, a rather deep invariant water layer was used throughout the experiment, and there was no phase transition taking place at the bottom of the tank. They both reported a nearly identical heat flux of approximately 340 W/m² independent of the initial water temperature. The discrepancy in reported q values (in Yen's work the melt layer was formed as melting progressed, and in Townsend's and Adrian's case there was only a liquid phase to begin with) are believed to be due to the real difference in the transfer processes involved in the experimental system.

HEAT TRANSFER STUDIES IN NONPLANAR GEOMETRIES

The most comprehensive and earliest theoretical study of melting free convective heat transfer, other than the horizontal geometries such as spheres and cylinders, was reported by

Merk (1954). Employing a third-order density-temperature polynomial of water density and applying the Von Karman-Pohlhausen integral method for the case of Pr >> 1, he successfully solved the boundary layer equation and developed a general Nusselt number ratio:

$$\frac{Nu}{Nu_o} = \left[\left(P_1 + \frac{6715}{13671} P_2 m + \frac{8471}{31031} P_3 n\right)\frac{[1+(S/2)]^3}{1-St}\right]^{1/4} \tag{16}$$

where S is the shape factor of the temperature profile and is connected to the Stefan number $St = c_p(T_m - T_\infty]/L$ as

$$S = -2 + \frac{3}{St} - \frac{3}{St}\sqrt{1 - \frac{4}{3} St} \tag{17}$$

or

$$St = \frac{6S}{(S+2)^2}, \tag{18}$$

where T_∞ is the bulk water temperature. The values of P_1, P_2, and P_3 are expressed as

$$P_1 = 1 - \frac{89}{217} S + \frac{19}{434} S^2 \tag{19}$$

$$P_2 = 1 - \frac{765}{1343} S + \frac{303}{2686} S^2 - \frac{19}{2686} S^3 \tag{20}$$

and

$$P_3 = 1 - \frac{6475}{8471} S + \frac{3537}{16942} S^2 - \frac{199}{8471} S^3 + \frac{19}{16942} S^4 \tag{21}$$

The values of m and n are defined respectively as

$$m = (\beta_2 + 3\beta_3 T_\infty)\theta_m / N\beta \tag{22}$$

$$n = \beta_3 \theta_m^2 / (N\beta_\infty) \tag{23}$$

where $\theta_m = T_m - T_\infty$ and N and β_∞ are defined as

$$N = 1 + \beta_1 T_\infty + \beta_2 T_\infty^2 + \beta_3 T_\infty^3 \tag{24}$$

and

$$\beta_\infty = (\beta_1 + 2\beta_2 T_\infty + 3\beta_3 T_\infty^2)/N \tag{25}$$

in which the βs are the coefficient in the formula for the specific volume of the water, i.e.

$$\frac{1}{\varrho} = \frac{1}{\varrho_o}(1 + \beta_1 T + \beta_2 T^2 + \beta_3 T^3). \tag{26}$$

Nu_o is the Nusselt number for the case of $St \approx m = n = 0$. Merk (1954) reported that for

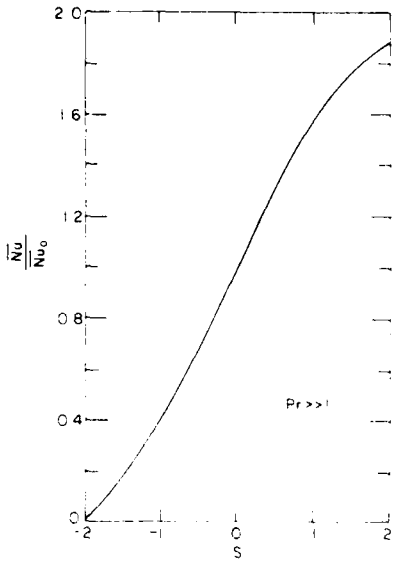

Figure 23. The influence of melting (S < 0) and solidification (S > 0) on the heat transfer in thermal convection for large values of the Prandtl number (after Merk 1954).

large values of the Prandtl number, neither the shape of the body nor the position on the surface influences the ratio Nu/Nu_o. Therefore this ratio can be replaced by $\overline{Nu}/\overline{Nu}_o$, and can be expressed by the following if only the effect of melting is considered (i.e. for $m = n = 0$)

$$\frac{\overline{Nu}}{\overline{Nu}_o} = \frac{1 - \frac{89}{217} S + \frac{19}{434} S^2}{1 - \frac{1}{2} S + \frac{1}{4} S^2} \left(1 + \frac{1}{2} S\right)^5 \tag{27}$$

Figure 23 is a graphic representation of eq 27; it clearly shows that for $S < 0$ or for melting, $\overline{Nu} < \overline{Nu}_o$, while for solidification, i.e. $S > 0$, $\overline{Nu} > \overline{Nu}_o$. For the case of no melting but with convective inversion, then $S = 0$ and hence $P_1 = P_2 = P_3 = 1$. Equation 26 becomes

$$\frac{\overline{Nu}}{\overline{Nu}_o} = (1 + 0.4912m + 0.2730n)^{1/4}. \tag{28}$$

By defining $\overline{Nu}_o$ for large values of the Prandtl number as

$$\overline{Nu}_o = C(GrPr)^{1/4} = C\left(\frac{gL^3}{\alpha \upsilon} \beta_\infty \theta_m\right)^{1/4}. \tag{29}$$

Equation 28 can be written as

$$f = \frac{\overline{Nu}}{\left(C \frac{gL^3}{\alpha \upsilon}\right)^{1/4}} = [\beta_\infty \theta_m (1 + 0.4912m + 0.2730n)]^{1/4} \tag{30}$$

where f is a dimensionless number. For small values of T_∞, $\beta_\infty \approx \beta_1 + 2\beta_2 T_\infty$, $m \approx \beta_2 \theta_m / \beta_\infty$, and $n \approx 0$, eq 30 can be simplified to

$$f = [1.509\beta_2 \; T_\infty - T_{iv} \; T_m - T_\infty \;]^{1/4} \tag{31}$$

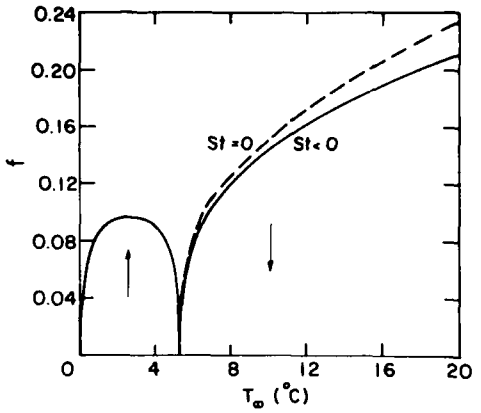

Figure 24. Convective inversion for melting ice in water of temperature T_∞. *The arrows indicate the direction of the flow along the surface. The dashed-dotted curve shows the behavior neglecting melting, while in the full curve the melting is taken into account (after Merk 1954).*

in which T_{iv} is the inversion temperature:

$$T_{iv} = -0.663 \frac{\beta_1}{\beta_2} - 0.326 T_m. \tag{32}$$

Using appropriate values of β_1 and β_2 and taking $T_m = 0°C$, Merk reported a value of $T_{iv} = 5.005°C$, indicating that the inversion temperature for melting ice in water is somewhat greater than $\approx 4°C$. The significance of the inversion temperature is clearly seen from eq 31 at $T_\infty = T_{iv}$, $\overline{Nu} = 0$, and the direction of the flow in the boundary layer along the surface of the body is inverted (for $T_\infty < T_{iv}$ the flow is upward and for $T_\infty > T_{iv}$ it is downward). Using the general eq 16, Merk derived the minimum Nusselt number at $T_{iv} = 5.30°C$ for $S = 0$ (no melting) and $T_{iv} = 5.31°C$ for $S < 0$ (with melting). Figure 24 shows the effect on the value of f (i.e. the value of $\overline{Nu}$) with and without melting with the convective inversion. It is clearly shown that the effect of melting is only appreciable for $T_\infty > T_{iv}$ and may be neglected for $T_\infty < T_{iv}$. Experimental results of Dumoré et al. (1953) and analytical results from the nonmelting vertical plate study by Ede (1955) generally confirmed Merk's findings.

Tkachev (1953), using photographic techniques, reported a minimum Nusselt number for melting ice cylinders at 5.5°C and was the first to notice the peculiar nature of the maximum density boundary layer. He suggested that under certain conditions the boundary layer might be split with a predominantly upward motion immediately adjacent to the ice surface and a region of downward motion outside this. Tkachev conducted melting experiments on spheres as well as on vertical and horizontal cylinders. Using the same initial cylinder diameters but with various bulk water temperatures he found that the coefficient of heat transfer is lowest for a water temperature of about 5.5°C. He correlated his data with the following dimensionless expressions as

$$Nu_{md} = 0.40(GrPr)_{md}^{1/4} \tag{33}$$

and

$$Nu_{md} = 0.104(GrPr)_{md}^{1/4} \tag{34}$$

for cylinders for the values in the range of $10^2 < GrPr < 10^7$ and $(GrPr)_{md} > 10^7$ respectively. The corresponding equations for spheres are

$$Nu_{md} = 0.54(GrPr)_{md}^{1/4} \tag{35}$$

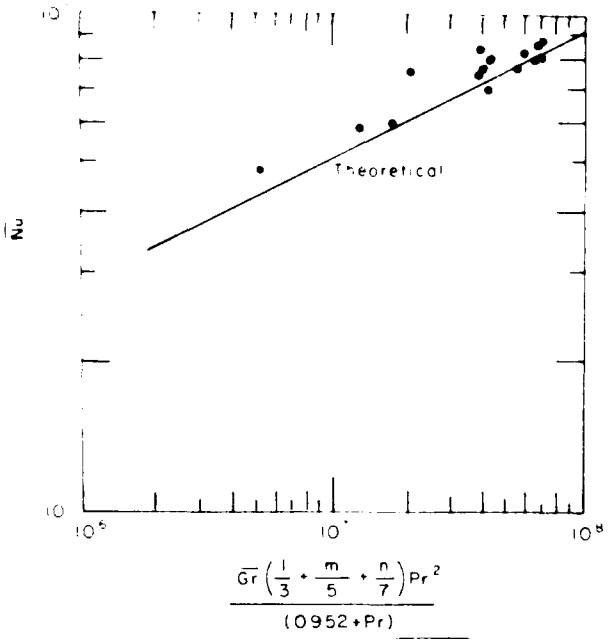

Figure 25. Comparison of theoretical (eq 37) and experimental $\overline{Nu}$ for unidirectional convection (after Schechter and Isbin 1958).

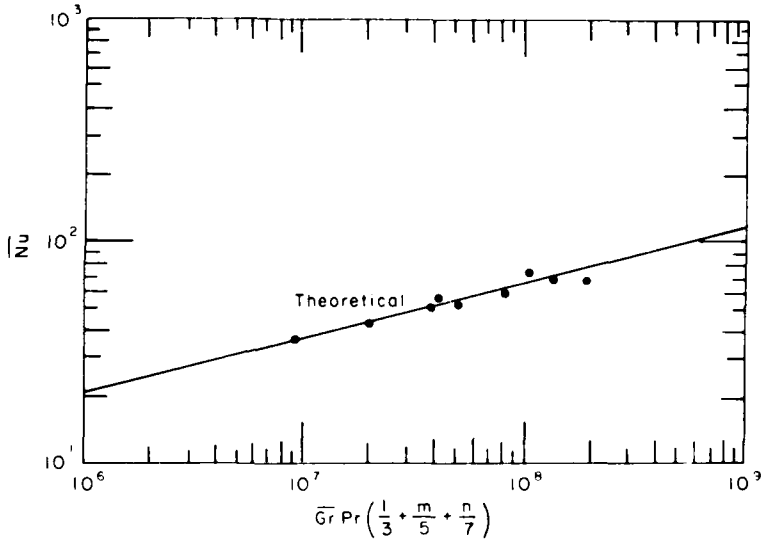

Figure 26. Comparison of theoretical (eq 38) and experimental $\overline{Nu}$ for inverted regime (after Schechter and Isbin 1958).

for laminar flow [$10^3 < (GrPr)_{md} < 10^7$] and

$$Nu_{md} = 0.135(GrPr)_{md}^{1/4} \tag{36}$$

for turbulent motion [$(GrPr)_{md} > 10^7$]. Subscript *md* represents the physical properties, and the diameter of the sphere or cylinder was evaluated at the arithmetic mean temperature [i.e. $(T_m + T_\infty)/2$] and diameter [i.e. $(d_o + d_f)/2$] where d_o and d_f are the initial and final diameter at the end of the experiment. Based on his experimental data, Tkachev further presented an expression for determining the time required for completing melting as

$$StFo_{md}Nu_{md} = 0.305. \tag{37}$$

The suggestion of split boundary layer flow was verified by the analytical and experimental work of Schecter and Isbin (1958), in which an isothermal, vertical, nonmelting plate was used. Figures 25 and 26 compare the theoretical and experimental results for the unidirec-

tional and inverted convections respectively. The theoretical curves in Figures 25 and 26 are given by

$$\mathrm{Nu} = 0.892\left[\frac{\overline{\mathrm{Gr}}\left(\frac{1}{3} + \frac{m}{5} + \frac{n}{7}\right)}{(0.952 + \mathrm{Pr})}\right]^{1/4} \mathrm{Pr}^{1/2} \tag{38}$$

and

$$\overline{\mathrm{Nu}} = 0.652\left[\overline{\mathrm{Gr}}\mathrm{Pr}\left(\frac{1}{3} + \frac{m}{5} + \frac{n}{7}\right)\right]^{1/4} \tag{39}$$

where m and n are defined in eq 22 and 23. They reported that a test of the type of region that will prevail for given conditions of plate and bulk temperature can be stated, i.e. if

$$\frac{1}{3} + \frac{m}{5} + \frac{n}{7} \geq 0,$$

there will be normal convection (unidirectional), and if

$$\frac{1}{3} + \frac{m}{5} + \frac{n}{7} < 0,$$

there will be inverted convection. They concluded that the heat transfer coefficient can be predicted for both regions with a deviation in Nusselt number of $\pm$ 10% provided the absolute value of $(1/3 + m/5 + n/7) > 0.05$ by use of eq 38 or 39, depending on the convective region. However, it should be noted that the boundary layer equations as approached either by the Von Karman-Pohlhausen integral method or by the similarity transformation method did not yield meaningful results under split-flow conditions.

To resolve this problem Vanier and Tien (1968) used an accurate numerical method to solve the similarity equations for a semi-infinite vertical plate at constant temperature T_w immersed in an indefinitely large volume of water at bulk temperature T_∞. They reported a new solution is necessary for every combination of T_w and T_∞. By obtaining several hundred such solutions, the authors were able to map out temperature zones for each flow regime. The split boundary layer was found to be confined to two distinct triangular regions within which the similarity equations become quite intractable. They confirmed the findings of Merk (1954) that the melting heat transfer rates were closely similar to the case of nonmelting.

Vanier and Tien (1970) conducted experimental work aimed at relating their numerical plate results to a more practical geometry of the sphere (including the effect of changing body configuration). This was also partially motivated by lack of detailed analysis and correlations of the experimental results on the melting of ice spheres and cylinders presented by Dumoré et al. (1953) and Tkachev (1953). They presented their results in a least-squares-fitted semiempirical equation as

$$\mathrm{Nu} = 2 + C(\mathrm{GrPr})^{1/4} \tag{40}$$

and found that for $T_\infty > 7°\mathrm{C}$, it appears that the results are not affected by the maximum density and the best value of C is 0.422 $\pm$ 0.006 in the range of $1.7 \times 10^6 < \mathrm{GrPr} < 2.4 \times 10^8$ (Fig. 27, curve b). However, for $T_\infty < 7°\mathrm{C}$, nearly the same value of C is found but with considerably more scattering (twice the standard deviation), indicating the need at least to incor-

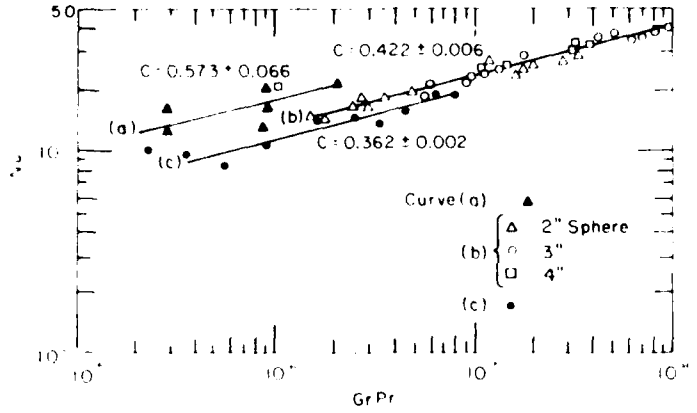

Figure 27. Nusselt number as function of Rayleigh number (GrPr) (after Vanier and Tien 1970).

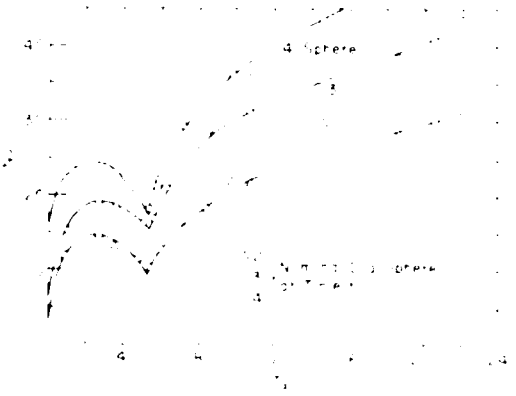

Figure 28. Nusselt number variation with bulk temperature for approximately constant sphere diameters (after Vanier and Tien 1970).

porate another parameter such as T_∞ to describe adequately the heat transfer under these conditions. This was done by separating the low temperature data into positive and negative deviations. For $T_\infty < 3.8°C$, Nu values are higher than expected (curve a), while for $4.1° < T_\infty < 7.1°C$, Nu values are too low (curve c). To check the one-quarter power assumption in eq 40, a two-parameter fit was carried out, resulting in

$$\mathrm{Nu} = 2 + 0.437(\mathrm{GrPr})^{0.248}, \tag{41}$$

which provides an excellent verification. However, if the Grashof number were calculated by using an arithmetic mean temperature basis of T_∞, the constant C was found to be 0.52 for $T_\infty > 14°C$. This provides a remarkable agreement with the results reported by Tkachev (1953). The effect of sphere diameter and maximum density on heat transfer can be seen in Figure 28. These curves are in general agreement with the flat plate results reported by Vanier and Tien (1968), which show a sharp minimum between $5° < T_\infty < 6°C$. To ascertain the effect of sphere diameter, Vanier and Tien (1970) proposed a correlation of the sphere results with those from theoretical analysis of a melting plate by

$$\overline{\mathrm{Nu}}_p/\overline{\mathrm{Nu}} = C(L/D)^{3/4} \tag{42}$$

where L and D are the characteristic height of the plate and the diameter of the sphere. The least-squares-fitted constant C was found to be 1.106 ± 0.144. The scaled-up experimental

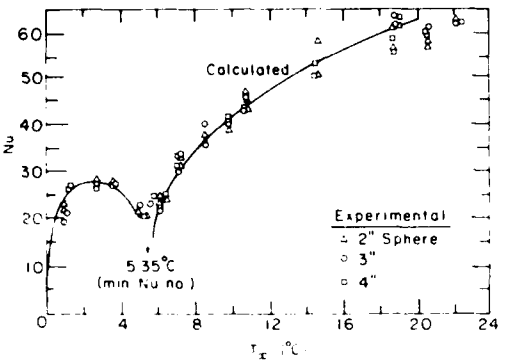

Figure 29. Correspondence between the melting of flat plates and spheres of ice (after Vanier and Tien 1970).

data are shown in Figure 29. This figure clearly means that a melting sphere behaves very similarly to a melting flat plate and that if all the transfer parameters are equal (including temperature, characteristic length, and surface area), about 11% more heat is transferred to the plate than to the sphere. This is the effect of curvature on the flow velocities and is in good agreement with the analytical results reported by Merk and Prins (1954) for nonmelting free convection systems without maximum density effects, i.e.

$$\overline{Nu}_p/\overline{Nu} = 1.14(L/D)^{3/4}. \tag{43}$$

The minimum Nusselt number for spheres occurs at $T_\infty = 5.35 \pm 0.2$°C, as compared to the value of 5.31°C based on Merk's (1954) theoretical results.

The most recent study of heat transfer and ice melting in ambient water near its density extremum was reported by Bendell and Gebhart (1976). In their experiment, a vertical ice slab (30.3 cm high, 14.8 cm wide, 3 cm thick initially) was immersed in water at a uniform bulk ambient temperature, T_∞. Figure 30 shows the experimental results along with the analytical results of Gebhart and Mollendorf (1978) and the results predicted with the Boussinesq approximation. Gebhart and Mollendorf's work is similar to that of Vanier and Tien (1968) except it gives a more accurate representation of the density-temperature of water. As Vanier and Tien pointed out, in the inversion region the validity of the simplest boundary layer theory becomes questionable. However, beyond that region, the experimental Nusselt number values were nearly equal to those predicted by theoretical analysis. Bendell and Gebhart (1976) reported that for a melting vertical ice surface, upflow occurred when $T_\infty \leq 5.6$°C. For $T_\infty \geq 5.5$°C, downflow was observed and was found to be in good agreement with earlier results. They found the minimum Nusselt number for the experimental temperature range $2.2° \leq T_\infty \leq 25.2$°C occurred at $T_\infty = 5.6$°C. In the immediate neighborhood of the

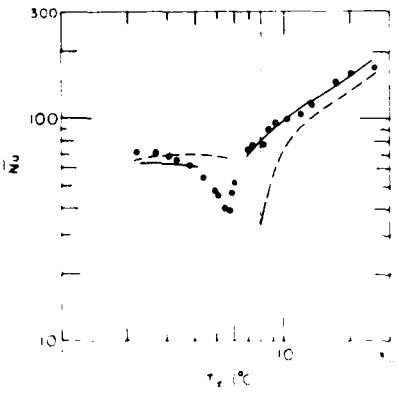

Figure 30. Variation of mean Nusselt numbers with ambient temperature T_∞ (0, experimental results). The solid curve is from the analytical work of Gebhart and Mollendorf (1978), the dashed curve is the prediction with the Boussinesq approximation (after Bendell and Gebhart 1976).

flow direction inversion T_{iv}, very slow flows exist with the effective Grashof number become very small, so the validity of the simplest boundary-layer theory becomes questionable; no theoretical results for this regime were found in the literature. In general, the theoretical results of Gebhart and Mollendorf after multiplying by a factor of $(0.102/0.303)^{1/4}$ (solid curve in Fig. 30) compared remarkably well with those reported by Vanier and tien (see solid curve in Fig. 29), even though a rather elaborate and more accurate density-temperature of water was claimed to be used in Gebhart and Mollendorf's study.

FORCED CONVECTIVE HEAT TRANSFER OVER A MELTING SURFACE

Yen and Tien (1963) were the first to investigate the problem of laminar heat transfer over a melting plate. With the assumption of a linear velocity profile ($v_x = cy$) and with coordinates fixed on the melting surface, the energy equation is given as

$$cy \frac{\partial T}{\partial x} + v_{yo} \frac{\partial T}{\partial y} = \alpha \frac{\partial^2 T}{\partial y^2} \tag{44}$$

where v_{yo} is the interfacial velocity. Equation 44 was solved by iteration process with the first approximation by letting $v_{yo} = 0$ and $X = (c/9\alpha x)^{1/3} y$. The first approximate solution is

$$\frac{T - T_m}{T_\infty - T_m} = \frac{\int_0^X \exp(-\delta^3) d\delta}{a_o} \tag{45}$$

where δ is a dummy variable and a_o is defined as $\int_0^\infty \exp(-\delta^3) d\delta$. The final solution can be written as

$$\frac{T - T_m}{T_\infty - T_m} = \frac{\int_0^X \exp\left(-\delta^3 + \frac{\beta\delta}{a_N}\right) d\delta}{a_N} \tag{46}$$

where a_N is the limiting value of the sequences of $a_n \int_0^\infty [\exp(-\delta^3 + \beta\delta)/a_{n-1}] d\delta$ as $n \to \infty$. The melting rate is given by

$$v_{yo} = \frac{\Phi}{a_N} \left(\frac{c}{9\alpha x}\right)^{1/3} \tag{47}$$

in which

$$\Phi = \frac{k(T_\infty - T_m)}{\varrho L}.$$

The Nusselt number is

$$\mathrm{Nu} = \left(\frac{i}{a_N}\right) \left(\frac{c}{9\alpha x}\right)^{1/3} . \tag{48}$$

The ratio of the Nusselt number with melting to that without melting and by neglecting factor $(c/9\alpha x)^{1/3}$ is

$$\psi(\beta) = \mathrm{Nu}/\mathrm{Nu}_o = a_o/a_N. \tag{49}$$

If a reasonable estimation of $c = \tau_w/\mu$ is given where τ_w is the wall shear stress, the ratio of the Nusselt number becomes

$$\theta(\beta) = \frac{Nu}{Nu_o} = \left(\frac{a_o}{a_N}\right)\left(\frac{\tau_w}{\tau_{wo}}\right)^{1/3} . \quad (50)$$

Since τ_w is proportional to the velocity gradient, and with the assumption that the distribution of the velocity profile is comparable to that of the temperature profile, eq 50 becomes

$$\theta(\beta) = Nu/Nu_o = (a_o/a_N)^{4/3}. \quad (51)$$

Figure 31 shows the effect of $\beta(= -St)$ on the values of $\psi(\beta)$ and $\theta(\beta)$. Table 3 shows the values of a_N as a unique function of β. From the numerical values of a_N, it becomes obvious that the surface heat flux reduces the steepness of the temperature gradient and consequently decreases the heat transfer coefficient. Figure 32 illustrates the effect of β on the temperature distribution. It clearly indicates that at the same value of X, the dimensionless temperature $T-T_m/T_\infty-T_m$ is lowered as β is increased from 0 to 1.

Table 3. Numerical values of a_N as a function of β (after Yen and Tien 1963).

$\beta(= -St)$	a_N
0.0	0.893
0.1	0.941
0.2	0.990
0.3	1.039
0.4	1.085
0.5	1.131
0.6	1.176
0.7	1.219
0.8	1.262
0.9	1.305
0.10	1.346

The assumption $v_x = cy$ simplified Yen and Tien's (1963) analysis, but it is known that for fluids of high Prandtl numbers the thermal boundary is not as thick as the velocity boundary layer. In view of this, Tien and Yen (1964) performed an additional analysis of the same

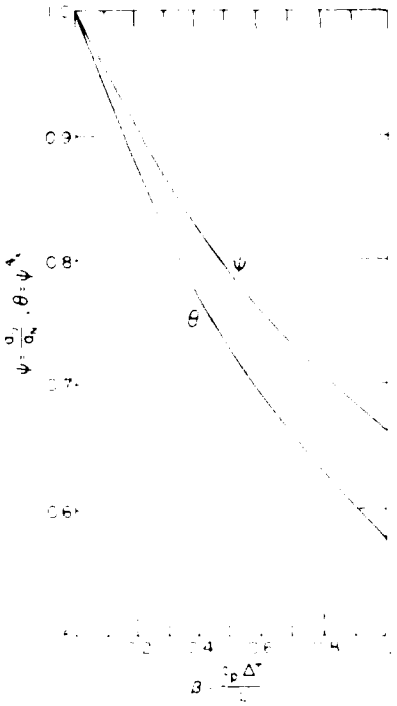

Figure 31. Relationship between ψ, θ, and β.

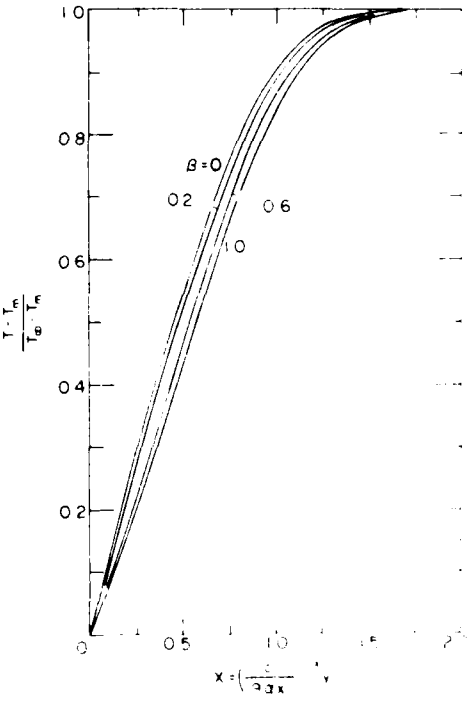

Figure 32. The effect of β on temperature distribution.

problem but proposed the portion of the velocity profile within the thermal boundary layer as

$$v_x = c(x)y. \tag{52}$$

The energy equation is solved as

$$T^*(\eta) = \frac{T-T_m}{T_\infty - T_m} = \frac{\int_0^\eta \exp\left(-\eta^3 + \frac{\omega}{a_N}\right)d\eta}{\int_0^\infty \exp\left(-\eta^3 + \frac{\omega}{a_N}\right)d\eta} \tag{53}$$

in which

$$\omega = \beta \frac{dT^*}{d\eta}\Big|_0 \tag{54}$$

and

$$\eta = y[c(x)]^{1/2}\{9\alpha\int_0^x [c(x)]^{1/2}\,dx\}^{-1/3}. \tag{55}$$

The Nusselt number is

$$\mathrm{Nu} = \left[\frac{1}{\int_0^\infty \exp\left(-\eta^3 + \frac{\omega}{a_N}\eta\right)}\right]^{1/3} \frac{\sqrt{c(x)}}{9\alpha\int_0^x \sqrt{c(x)}\,dx}. \tag{56}$$

The ratio of the Nusselt number is now

$$\frac{\mathrm{Nu}}{\mathrm{Nu}_o} = \frac{\int_0^\infty \exp(-\eta^3)d\eta}{\int_0^\infty \exp(-\eta^3 + \frac{\omega}{a_N}\eta)d\eta} \sqrt{\frac{c(x)}{c(x)_o}} \left[\frac{\int_0^x \sqrt{c(x)_o}dx}{\int_0^x \sqrt{c(x)}dx}\right]^{1/3} \tag{57}$$

The first part on the right side of eq 57 is equal to $\psi(\beta) = a_N$, and if it is assumed that the effect of melting on the temperature gradient is comparable to the effect on the velocity gradient, then eq 57 is equivalent to eq 51, indicating that results obtained based on a rather restricted assumption are applicable to more realistic cases.

Pozvonkov et al. (1970) also conducted an analytical study on heat transfer at a melting flat surface under the conditions of forced convection and laminar boundary layer. In their study, the boundary layer equations were solved with the assumptions of constant thermal-physical properties of the fluid, independence of the ratio of momentum to thermal boundary layer thickness (δ/δ_t) in the direction of flow, and a fourth-degree polynomial representation of the velocity and temperature distribution. The ratio of the local Nusselt number with melting to that without melting is given as

$$\frac{\mathrm{Nu}_x}{\mathrm{Nu}_{xo}} = \sqrt{\left(\frac{a}{2}\frac{1}{1+\frac{1}{k_f}}\right)}\sqrt{\frac{\delta_t^{**}}{\delta_{to}^{**}}} \tag{58}$$

in which k_f is the Kutateladze number (= $-1/\mathrm{St}$), a is expressed in terms k_f by

$$a = 3\left[\sqrt{\left(k_f^2 + \frac{4}{3}k_f\right)} - k_f\right], \tag{59}$$

and

$$\delta_t^{**} = \int_0^1 \left(1 - \frac{T}{T_\infty}\right)\frac{u}{u_\infty}\, d\eta \tag{60}$$

where T/T_∞ and u/u_∞ are the dimensionless thermal and velocity boundary-layer distributions. The value of δ_{to}^{**} is for the case when there is no melting. To evaluate the values of δ_t^{**} and δ_{to}^{**}, the values of σ_{to}^{**} ($\delta^{**} = \delta_o^{**}$ when there is no melting) has to be evaluated from

$$\delta^{**} = \int_0^1 \left(1 - \frac{u}{u_\infty}\right)\frac{u}{u_\infty}\, d\eta \tag{61}$$

where $\eta = y/\delta t$ or $\eta = y/\delta$. The value of δ_o^{**} can be found directly from eq 61, but the value of δ_{to}^{**} will contain the unknown boundary-layer thickness ratio $\epsilon_o = \delta_{to}/\delta_o$. By retaining only the first power in ϵ_o in the expression δ_{to}^{**}, the first approximation of ϵ_o can be evaluated from

$$\delta_o/\delta_{to} = \delta_{to}^{**}/\delta_o^{**}\sqrt{\text{Pr}} \tag{62}$$

for the case of no melting. Equation 62 is reduced from the general expression of

$$\frac{\delta}{\delta_t} = \sqrt{\left(\frac{\delta_t^{**}}{\delta^{**}}\right)}\,\frac{\sqrt{\frac{A}{a}}}{\sqrt{1 + \frac{1}{k_f}}}\sqrt{\text{Pr}} \tag{63}$$

where

$$A = \frac{2}{1 + \frac{\lambda_o}{\epsilon\sqrt{\text{Pr}}}} + \frac{6\lambda_o}{\epsilon\,\text{Pr}}$$

$$a = 3\sqrt{k_f^2 + \frac{4}{3}k_f} - k_f \tag{64}$$

in which $\lambda_o = a/6k_f$ and $\epsilon = \delta_t/\delta$. By repeated application of eq 61 and the expression for δ_{to}^{**} derived from eq 60, a final value of

$$\delta_o/\delta_{to} \text{ (or } \epsilon_o = \delta_{to}/\delta_o)$$

can be found. This final value of ϵ_0 is used as a first approximation to evaluate the values of δ_t^{**} and δ^{**} from eq 60 and 61. Equation 63 is then used to compute a new value of δ/δ_t (or $1/\epsilon$) and is used again in eq 60 and 61 to compute a second set of values of δ_t^{**} and δ^{**}. A new value of δ/δ_t is computed from eq 63 and is repeated until this final value is nearly identical to the previously calculated one. The results from this rather complicated boundary-layer integral analysis are compared in Figure 33 with the much simplified work by Yen and Tien (1963).

The effect of melting on forced convection heat between a melting body and the surround-

ing fluid was studied quantitatively from the points of view of boundary layer theory, film theory, and penetration theory by Tien and Yen (1965).

In the case of boundary layer theory, exact solutions of the equations of motion, energy, and continuity were obtained and the relation between the ratio of θ_T (= h/h_0) of heat transfer coefficient with melting to without melting was derived in terms of the parameter β(= $-$St) as

$$\theta_T = \left(\frac{K \cdot \mathrm{Pr}}{T^{*\prime}(0,\mathrm{Pr},0)}\right)/\beta \qquad (65)$$

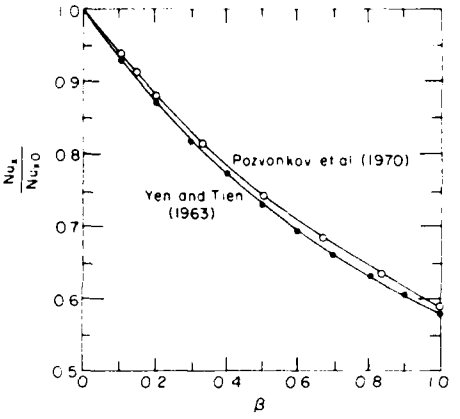

Figure 33. Comparison of Nu_x/Nu_{xo} vs β.

where T^* is the derivative with η of the dimensionless temperature identically defined in eq 53 but with η defined as

$$\eta = (y/2)(\nu_\infty/\upsilon_x)^{1/2}.$$

The parameter K is given as

$$K = (\beta/\mathrm{Pr})T^{*\prime}(0,Pr,K).$$

Numerical values of $[K \cdot Pr/T^{*\prime}(0,Pr,K)]$ as functions of θ_T have been compiled by Stewart (1950).

In the analysis based on film theory, the resistance to the interphase transport phenomenon is assumed to be confined to a thin layer of stagnant film immediately adjacent to the solid boundary. The model is assumed to be one-dimensional (perpendicular to the surface) and of steady state. The parameter θ_T is found to be

$$\theta_T = \frac{\ln(1+\beta)}{\beta} \qquad (66)$$

In the penetration model analysis, it is hypothesized that the transport process is affected by small eddies of the fluid in a turbulent field coming into contact with the interfaces. Since in most cases the duration of contact is rather short, the eddy may be treated as a semi-infinite solid, and a transient-state heat conduction equation can be used to describe the energy transfer process. A solution was attained, and the ratio θ_T is expressed as

$$\theta_T = 1/(1-\mathrm{erf}\,\phi)\,\mathrm{erf}(\phi^2) \qquad (67)$$

in which ϕ is related to β by

$$(1-\mathrm{erf}\,\phi)\sqrt{\pi}\,\phi\exp(\phi^2) = -\beta. \qquad (68)$$

Figure 34 shows the effect of β on the values of θ_T from the considerations of boundary, film, and penetration theory along with the works reported by Yen and Tien (1963) and Merk (1954). Although the quantitative results differ, they all show the same qualitative trend and indicate that the process of phase transition (melting) inhibits the heat transfer rate. The results based on the Leveque solution agree with those based on boundary layer

theory for small values of β but deviate from each other as β increases. This is expected since the solution obtained by Yen and Tien, in a sense, is an asymptotic solution of that based on boundary layer theory for small β. The difference in results based on the boundary, film, and penetration models requires that caution be exercised in selecting among these results for practical applications.

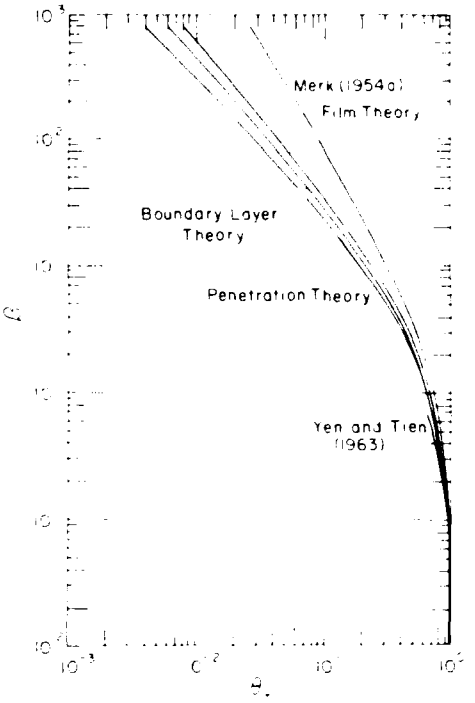

Figure 34. Comparison of various theories: the effect of β on θ_T (after Tien and Yen 1965).

DISCUSSIONS AND CONCLUSIONS

This review covers only the problems associated with the anomalous density-temperature relation of water. The discussion and conclusion are grouped into three sections, i.e. 1) onset of convection, 2) temperature structure and natural convective heat transfer, and 3) laminar forced convective heat transfer.

Onset of convection

The criterion of the onset of convection of a water layer that contains a density extremum was found both experimentally (Yen 1968, Yen and Galea 1969) and analytically (Veronis 1963, Sun et al. 1969, Merker et al. 1979) to be not a constant value, as in the classical Bénard problem, but dependent on the thermal boundary conditions (if the layer is formed by phase transition, then one of the thermal boundaries is at the ice melting point, i.e. $T_m = 0°C$). The experimental values were compared with analytical values very favorably as shown in Figure 12 in terms of Ra_c experimental vs Ra_c theoretical and in Figure 13 as Ra_c vs T_1 or T_2 explicitly and from which it can be concluded that in the case of melting from the top, the higher the values of T_2, the greater Ra_c becomes, or in other words the farther removed temperature T_2 is from 4°C, the less prone the layer is to the onset of convection. On the other hand, in the case of melting from below, as temperature T_1 increases, Ra_c reduces exponentially and approaches the value $\approx$ 1708 asymptotically as reported in the classical Bénard problem. This is evident from the fact that as T_1 becomes higher and higher, the buoyancy forces created by temperature difference $\Delta T = T_1 - T_{max}$ possess a much stronger influence on the layer stability than the effect produced by the density extremum (i.e. $\approx$ 4°C), and subsequently the continuously forming layer behaves like a normal fluid (i.e. there is a monotonic density-temperature relationship) as in the Bénard problem. On the other hand, as T_1 decreases and approaches the temperature of the density extremum ($\approx$ 4°C), Ra_c increases and approaches the limiting value of infinity. This is also expected, since if T_1 is maintained at $\approx$ 4°C, the water has its highest density at the lower boundary and the water layer will always remain stable.

In the case of a water layer formed by melting ice from above, the trend of variation of Ra_c with boundary temperature is just reversed. The higher the temperature T_2, the greater Ra_c becomes. This can be explained by noting that if T_2 is maintained in the range $0 < T_2 \leq 4°C$, the entire layer is unstable because the higher density water will overlie the less dense water underneath, and will consequently result in lower Ra_c values. If T_2 is maintained at a higher temperature than 4°C, only a fraction of the layer ($= 4H/T_2$) is potentially unstable, so the layer is less prone to onset of convection. It seems that the Ra_c value grows greater and

greater as the effect of the density extremum becomes less and less pronounced. It is also interesting to note that the two Ra_c curves intersect at exactly $T_1 = T_2 = 8°C$, which clearly indicates that under this particular thermal condition, these two systems are identical and have a unique Ra_c value regardless of how the water layer was formed.

Temperature structure and natural convective heat transfer

The most striking phenomenon of the temperature distribution either in the constant water layer depth (Townsend 1964, Myrup et al. 1970) or in the continuously growing layer from melting ice (Yen 1984) is the formation of a nearly constant temperature region that eventually expands to two-thirds of the entire layer depth. The only significant difference observed is that the temperature in the constant temperature region in the water layer formed by melting ice from below depends on the boundary temperature T_1 (see Fig. 19c), but is a fixed value ($\approx 3.2°C$) independent of the imposed upper boundary temperature T_2 (Fig. 21c) in the water layer formed by melting from the top. This is identical to the temperature structure measured in the rather deep and constant depth water layer reported by Townsend (1964) (Fig. 17a) and Myrup et al. (1970).

The heat flux for melting from the top is found to be a weak function of T_2 and can be expressed as $q = 177\ (T_2)^{0.303}$ in which q is given in W/m². However, in melting from below, the heat flux is found to be strongly dependent on T_1 and can be approximated by $q = -1900 + 315(T_1)$. This is because as T_1 is maintained at a higher value there will be a stronger current of mixing in the constant temperature region, thus reducing the laminar layer thickness on the lower boundary and the upper water/ice interface and increasing the heat transfer rate. On the other hand, the effect of T_2 on heat transfer is much weaker because there is a stable layer overlying the expanding unstable region and, in addition, the buoyancy force is created merely by a temperature difference of 4°C (i.e. $4°C - 0°C = 4°C$). The works of Townsend (1964) and Adrian (1975) are similar to the work of melting ice from the top, and they reported nearly identical heat fluxes of approximately 340 W/m², which is somewhat lower than those obtained from the melting experiment. The discrepancy can probably be attributed to the unsteady nature of the melting experiment (i.e. the layer depth is initially at zero and it deepens as the melting progresses).

The works of Tkachov (1953), Merk (1954), Schechter and Isbin (1958), Vanier and Tien (1968, 1970), Bendell and Gebhart (1976), and Gebhart and Mollendorf (1978) were conducted either theoretically or experimentally and were aimed at classifying the implication of the density extremum on the heat transfer characteristics of a melting as well as a nonmelting system. Tkachov was the first to suggest that under certain thermal conditions the boundary layer might be split, with a predominantly upward motion immediately adjacent to the ice surface and a region of downward motion outside this. Based on his experimental work on ice spheres and vertical and horizontal cylinders, he reported that the heat transfer coefficient is lowest at a T_∞ of about 5.5°C. Merk was the first to take up this moving boundary problem analytically; he solved it with an approximation method. For the case of no melting and with a small value of T_∞, he reported the inversion temperature to be at $\approx 5.005°C$. Based on a rather complete calculation (i.e. without the limitation on T_∞), Merk reported the inversion temperature to be around 5.30°C for no melting and 5.31°C with melting; he further indicated that the effect of melting is only appreciable for $T_\infty > T_{iv}$ and may be neglected for $T_\infty < T_{iv}$ (Fig. 24).

The analytical work of Vanier and Tien (1968) also reported the existence of three types of flow regions, i.e. laminar upward, downward, and dual flow (sometimes termed "inverted" or "split"), as well as regions of no solution. These regions are determined by specific combinations of T_w and T_∞. Their computed results are found to be consistent with the observations by Tkachev (1953), the analytical and experimental works of Schecter and Isbin (1958),

and the analytical results of Merk (1954) as well as the experimental results of Dumoré et al. (1953). These analytical findings were verified with their experimental work on melting spheres similar to those reported by Tkachev and Dumoré et al. A minimum heat flux occurred around $T_{iv} = 5.35 \pm 0.2°C$ as compared with Merk's 5.31°C and Tkachev's 5.5°C. Their findings are also in good agreement with the most recent work of Bendell and Gebhart (1976). Based on the melting of vertical ice plates, they reported an inversion temperature of 5.6°C. Gebhart and Mollendorf (1978), however, claimed to have used a more elaborate and accurate density-temperature representation, and their results are comparable with those reported by Vanier and Tien (1968), even though a less complex density-temperature relation was used.

Laminar forced convective heat transfer

Based on the limited analytical work reported on forced convective heat transfer over a melting surface, it can be concluded that the interfacial velocity resulting from phase transition tends to retard heat transfer. From the most simplistic approach to this problem, Yen and Tien (1963) found the ratio of the Nusselt number with melting to that without melting to be a strong function of $\beta[= c_p(T_\infty - T_m)/L = -\mathrm{St}]$ (Fig. 31). This result was in good agreement with those reported by Pozvonkov et al. (1970) from a rather complicated integral solution of the transport equations (Fig. 33). The reduction of the heat transfer rate is attributed to the lowering of the temperature gradient and its equivalent to the case of mass injection through the laminar layer into the mainstream. This evidence (Fig. 34) was further demonstrated by Tien and Yen (1965), based on their quantitative analysis of this moving boundary problem with classical boundary, film, and penetration theory.

LITERATURE CITED

Adrian, R.J. (1975) Turbulent convection in water over ice. *Journal of Fluid Mechanics,* **698**: 753-781.

Bénard, H. (1900) Les tourbillons cellulaires dans une nappe liquid. *Revue Générale des Sciences Pures et Appliqués,* **11**: 1261-1271.

Bendell, M.S. and B. Gebhart (1976) Heat transfer and ice melting in ambient water near its density extremum. *International Journal of Heat and Mass Transfer,* **19**: 1081-1087.

Boger, D.V. and J.W. Westwater (1967) Effect of buoyancy on the melting and freezing process. *Journal of Heat Transfer,* **69**: 81-89.

Chandrasekhar, S. (1961) *Hydrodynamic and Hydromagnetic Stability.* Oxford: Clarendon Press.

Dumoré, J.M., H.J. Merk and J.A. Prins (1953) Heat transfer from water to ice by thermal convection. *Nature,* **172**: 460-461.

Ede, A.J. (1955) The influence of anomalous expansion on natural convection in water. *Applied Scientific Research,* **5**: 458-460.

Gebhart, B. and J.C. Mollendorf (1978) Buoyancy-induced flows in water under conditions in which density extrema may arise. *Journal of Fluid Mechanics,* **89**(4): 673-707.

Globe, S. and D. Dropkin (1959) Natural convection heat transfer in liquids confined by two horizontal plates and heated from below. *Journal of Heat Transfer,* **81**: 24-28.

Jeffreys, H. (1926) The stability of a layer of fluid heated below. *Philosophical Magazine,* **2**: 833-844.

Legros, J.C., D. Longree and G. Thomas (1974) Bénard problem in water near 4°C. *Physica,* **72**: 410-414.

Merk, H.J. (1954) The influence of melting and anomalous expansion on the thermal convection in laminar boundary layers. *Applied Science Research,* **III**(A4): 435-452.

Merk, H.J. and J.A. Prins (1954) Thermal convection in laminar boundary layers. *Applied Science Research,* **III**(A4): 207-223.

Merker, G.P., P. Wass and U. Grigull (1979) Onset of convection in a horizontal water layer with maximum density effects. *International Journal of Heat and Mass Transfer,* **22**: 505-515.

Myrup, L., D. Gross, L.S. Hoo and W. Goddard (1970) Upside down convection. *Weather,* **25**: 150-157.

Pozvonkov, F.M., E.F. Shurgalskii and L.S. Akselrod (1970) Heat transfer at a melting flat surface under conditions of forced convection and laminar boundary layer. *International Journal of Heat and Mass Transfer,* **13**: 957-962.

Rayleigh, Lord (1916) On convective currents in a horizontal layer of fluid when the higher temperature is on the underside. *Philosophical Magazine,* **32**, 529-546.

Schechter, R.S. and H.S. Isbin (1958) Natural convection heat transfer in regions of maximum fluid density. *American Institute of Chemical Engineers Journal,* **4**: 81-89.

Schmidt, E. and P.L. Silveston (1959) Natural convection in horizontal liquid layers. *Chemical Engineering Symposium Series,* **55**(29): 163-169.

Stewart, W.E. (1950) Interaction of heat, mass and momentum transfer. D.Sc. dissertation, Massachusetts Institute of Technology.

Sun, Z.-S., C. Tien and Y.-C. Yen (1969) Thermal instability of a horizontal layer of liquid with maximum density. *American Institute of Chemical Engineers Journal,* **15**: 910-915.

Tien, C. and Y.-C. Yen (1964) An additional note on the modified Leveque problem. *Journal of Geophysical Research,* **69**: 1672-1673.

Tien, C. and Y.-C. Yen (1965) The effect of melting on forced convection heat transfer. *Journal of Applied Meteorology,* **4**: 523-527.

Tkachev, A.G. (1953) Heat exchange in melting and freezing of ice. In *Problems of Heat Transfer During a Change of State: A Collection of Articles.* Moscow: Translated from a publication of the State Power Press, AEC-Tr-34-5, p. 169-178.

Townsend, A.A. (1964) Natural convection in water over an ice surface. *Quarterly Journal of the Royal Meteorological Society,* **90**: 248-259.

Vanier, C.R. and C. Tien (1970) Free convection melting of ice spheres. *American Institute of Chemical Engineers Journal,* **16**: 76-82.

Veronis, G. (1963) Penetrative convection. *Astrophysical Journal,* **137**: 641-663.

Yen, Y.-C. (1968) Onset of convection in a layer of water formed by melting ice from below. *Physical Fluids,* **11**: 1263-1270.

Yen, Y.-C. (1980) Free convection heat transfer characteristics in a melt layer. *Journal of Heat Transfer,* **102**: 550-556.

Yen, Y.-C. (1984) Temperature structure and interface morphology in a melting ice-water system. In *Frontiers in Hydrology.* Water Resources Publications, p. 305-325.

Yen, Y.-C. and F. Galea (1969) Onset of convection in a water layer formed continuously by melting ice. *Physics of Fluids,* **12**: 509-516.

Yen, Y.-C. and C. Tien (1963) Laminar heat transfer over a melting plate, the modified Leveque problem. *Journal of Geophysical Research,* **68**: 3673-3678.

Yen, Y.-C. and C. Tien (1971) Heat transfer at a melting flat surface under conditions of forced convection and laminar boundary layer. *International Journal of Heat and Mass Transfer,* **14**: 1975-1976.

A facsimile catalog card in Library of Congress MARC format is reproduced below.

Yen, Yin-Chao

Thermal instability and heat transfer characteristics in water/ice systems / by Yin-Chao Yen. Hanover, N.H.: U.S. Army Cold Regions Research and Engineering Laboratory; Springfield, Va.: available from National Technical Information Service, 1987.

vii, 43 p., illus.; 28 cm. (CRREL Report 87-22.)

Bibliography: p. 32.

Prepared for Office of the Chief of Engineers by U.S. Army Cold Regions Research and Engineering Laboratory, Hanover, N.H.

1. Density inversion. 2. Heat transfer. 3. Ice. 4. Natural convection. 5. Thermal instability. 6. Water. I. United States Army. Corps of Engineers. II. Cold Regions Research and Engineering Laboratory. III. Series: CRREL Report 87-22.

END

DATE

FILMED

APRIL

1988

DTIC